June 2025, Tarragona

UNIVERSITAT ROVIRA i VIRGILI

DEGREE IN BIOCHEMISTRY AND MOLECULAR BIOLOGY

FINAL DEGREE PROJECT

Evaluation of recombinant lysosomal acid lipase role on atherosclerosis biomarkers of a LAL-D patient

Ainhoa Guerrero Ramírez

Academic tutor:

Ricardo Rodríguez Calvo, PhD

Department of Biochemistry and Biotechnology

Rovira i Virgili University, Tarragona

Professional tutors:

Josep Ribalta Vives, PhD
Josefa Girona Tell, PhD

Department of Medicine and Surgery

Rovira i Virgili University, Tarragona

Project based on the results obtained during my curricular practices conducted in IISPV (Institut d'Investigació Sanitària Pere Virgili), under the supervision of Dr. Josep Ribalta Vives and Dr. Josefa Girona Tell.

TABLE OF CONTENTS

1. ABBREVIATIONS

ACAT: Acyl-CoA-cholesterol acyltransferase

ADA: Anti-drug antibodies

ALT: Alanine aminotransferase

AST: Aspartate aminotransferase

CCL18/PARC: chemokine (C-C motif) ligand 18/pulmonary and activation-regulated chemokine

CE: Cholesterol esters

CESD: Cholesterol ester storage disease

ER: Endoplasmic reticulum

ERT: Enzyme replacement therapy

FA: Fatty acids

FC: Free cholesterol

HDL: High-density lipoprotein

HDL-C: High-density lipoprotein cholesterol

HLH: Hemophagocytic lymphohistocytosis

HMG-CoA: Hydroxymethylglutaryl-coenzyme A

IL-1β: Interleukin-1 beta

LAL: Lysosomal acid lipase

LAL-D: Lysosomal acid lipase deficiency

LCN2: Lipocalin-2

LDL: Low-density lipoprotein

LDL-C: Low-density lipoprotein cholesterol

LIPA: Lipase A, Lysosomal Acid Type

LRP1: Low density lipoprotein receptor-related protein 1

MAPK: p38 mitogen-activated protein kinase p38 mitogen-activated protein kinase

NMR: Nuclear magnetic resonance

PBMC: Peripheral blood mononuclear cell

PBS: Phosphate-buffered saline

SREBP: Sterol regulatory element binding protein

TFEB: Transcription factor EB

TG: Triglycerides

uCRP: Ultra sensible C-reactive protein

VLDL: Very-low-density lipoprotein

VLDL-C: Very-low-density lipoprotein cholesterol

WD: Wolman disease

4-MU: 4-methylumbelliferone

2. ABSTRACT

Lysosomal Acid Lipase Deficiency (LAL-D) causes lipid accumulation, liver dysfunction, and early atherosclerosis. This study evaluated whether Enzyme Replacement Therapy (ERT) with Sebelipase α improves atherosclerotic profile beyond lipid normalization. Lipid and hepatic profiles, macrophage lipid uptake, and inflammation-related biomarkers were assessed in a LAL-D patient under ERT and a healthy control. ERT normalized lipid levels and reduced inflammatory markers (GGT, LCN2), though E-selectin remained elevated. LAL-D macrophages showed reduced lipid uptake and inflammation, suggesting lower foam cell formation. These results support Sebelipase α's therapeutic effects, but larger studies are needed to validate findings and assess residual atherosclerotic risk.

3. INTRODUCTION

3.1. Lysosomal Acid Lipase Deficiency

Lysosomal acid lipase deficiency (LAL-D) (OMIM 278000) is an ultra-rare, autosomal-recessive lysosomal storage disease caused by a pathogenic mutation of the Lipase A, Lysosomal Acid Type (LIPA) gene, leading to an inactive or defective LAL activity (de las Heras et al. 2024). LAL is responsible for the catalysis of the intralysosomal hydrolysis of cholesterol esters (CE) and triglycerides (TG) that contain the low-density lipoprotein cholesterol (LDL-C); for that reason, this condition leads to a progressive lysosomal lipidic accumulation as a result of impaired LAL activity to hydrolyze the lipoprotein. In LALD, when CE are not adequately degraded in the lysosomes, cells (especially hepatocytes) detect low levels of free cholesterol. This triggers a compensatory response that stimulates the synthesis and release of cholesterol-rich lipoproteins, thus increasing circulating cholesterol. Lipidic accumulations take place in lysosomes of the cells where low-density lipoprotein (LDL) receptors are located, especially hepatocytes, adrenal glands, intestines, and cells of the macrophage-monocyte system (Bernstein et al. 2013) and give rise to different clinical manifestations involving multiple organs based on LAL activity level.

Wolman disease (WD) is a neonatal/infantile-onset and fulminant phenotype with complete deficiency or less than 1% of normal LAL activity that results in a massive accumulation associated with high mortality and has a rapid course, with a prevalence of approximately 1 per 350,000 live births. In the other side, cholesterol esters storage disease (CESD) is a later-onset subtype that is present in infancy to adulthood based on the LAL activity, which ranges between 1% to 12% of normal LAL activity and has a prevalence of approximately 1 per 300,000 individuals (de las Heras et al. 2024). Although the later-onset subtype is less fulminant, it can also lead to hepatic fibrosis and cirrhosis, atherosclerosis and premature cardiovascular disease and early death as the infant-onset subtype as a direct consequence of the ectopic lysosomal lipid accumulation and the elevation of lipidic profile. The accumulation of lipids can activate macrophages, which can become foam cells, leading to atherosclerosis and systemic inflammation.

Diagnosis, due to the lack of specificity of the symptoms and the low prevalence, can be challenging. It begins with a biochemical suspicion as a consequence of the dyslipidemia and hypertransaminemia (Wilson and Patni 2000), being the principal clinical manifestations of the disease. The determination of LAL activity from a sample of dried blood is a reliable and reproducible diagnostic procedure, although it does not allow differentiation between LAL-D of infantile onset and late onset (Hamilton et al. 2012).

The use of plasma biomarkers such as alanine amino transferase (ALT), aspartate amino transferase (AST) and total LDL are commonly used in the management of LAL-D to determine liver failure. Recent studies show that liver-derived Lipocalin-2 (LCN2) is a prognostic factor in a series of patients with acute-on-chronic liver failure (Chen et al. 2020).

As a direct consequence of the disease, biomarkers of inflammatory processes and oxidative stress are used (Guerreiro, Deon, and Vargas 2023). Regarding inflammation,

plasma chemokine (C-C motif) ligand 18/pulmonary and activation-regulated chemokine (CCL18/PARC) levels are elevated. These are released by activated macrophages, and their concentration is also elevated in other diseases such as lysosomal deposit and atherosclerosis, therefore, C-reactive protein (CRP) is also used to monitor inflammation. Oxidation includes oxysterols such as 7-ketocholesterol and cholestane-3β,5α,6β-triol which at elevated levels contribute to alterations in cholesterol metabolism (Pajares et al. 2015). Although they are not diagnostic measures, they are used to follow up patients with LAL-D, in the same way as imaging tests, biopsies or histological specimens.

Persistent dyslipidemia, a common manifestation in LAL-D patients, is associated with elevated total cholesterol levels, elevated LDL-C and ApoB and decreased high-density lipoprotein cholesterol (HDL-C) and is used also as a routine biomarker. That condition is associated with atherosclerosis and, consequently, premature cardiovascular disease. Furthermore, the activation of macrophages leads to the release of proinflammatory molecules such as enzymes or cytokines that can promote atherosclerosis, such as the biomarkers released by macrophages CCL18/PARC (Pajares et al. 2015).

LAL-D treatment is carried out by two fundamental pillars which are, on the one hand, a low-fat diet, as a substrate reduction therapy that leads to an increase in lysosomal disposition and, on the other hand, enzyme replacement therapy by means of the exogenous administration of the recombinant LAL enzyme, named Sebelipase α (Kanuma©, Alexion Pharmaceuticals, Inc., Cheshire, CT, USA). Sebelipase α is a recombinant human LAL that is produced in egg white from transgenic *Gallus gallus domesticus* hens. The attached mannose-6-phosphate residue facilitates its uptake into the lysosomes of hepatocytes and macrophages where it can subsequently hydrolyze cholesteryl esters and triglycerides (Malinová et al. 2020;Erwin 2017). In the case of the infantile-onset phenotype, treatment should be initiated as soon as possible to ensure survival, with a dosage of up to 5mg/kg of weight (Jones et al. 2017), while for the CESD phenotype the recommended dosage is 1mg/kg to 3mg/kg infused every two weeks (Malinová et al. 2020). Lipid-lowering agents also have a major role in later-onset subtype (Camarena et al. 2017; Chuang et al. 2014). As a result of the treatment, the lipid profile and liver injury markers are significantly improved.

3.1.1. Lysosomal Acid Lipase

LAL (EC 3.1.1.13; Uniprot: P38571) is the key enzyme for hydrolysis of CE and TG, especially, of lipoproteins in lysosomes taken up by receptor-mediated endocytosis. Is a 46 kDa glycoprotein encoded by lipase A (LIPA gene) and is the only known intracellular lipase active at an acidic pH (3.9-5.0) (Dubland and Francis 2015). After undergoing co-translational glycosylation in the endoplasmic reticulum (ER) and attachment of mannose-6-phosphate residues in the Golgi apparatus, LAL is targeted to pre-lysosomal compartments resulting in a 399-aminoacid mature protein (Korbelius et al. 2023). Modifications including glycosylation sites, fold, α-helices and β-strands are represented in Figure 1.

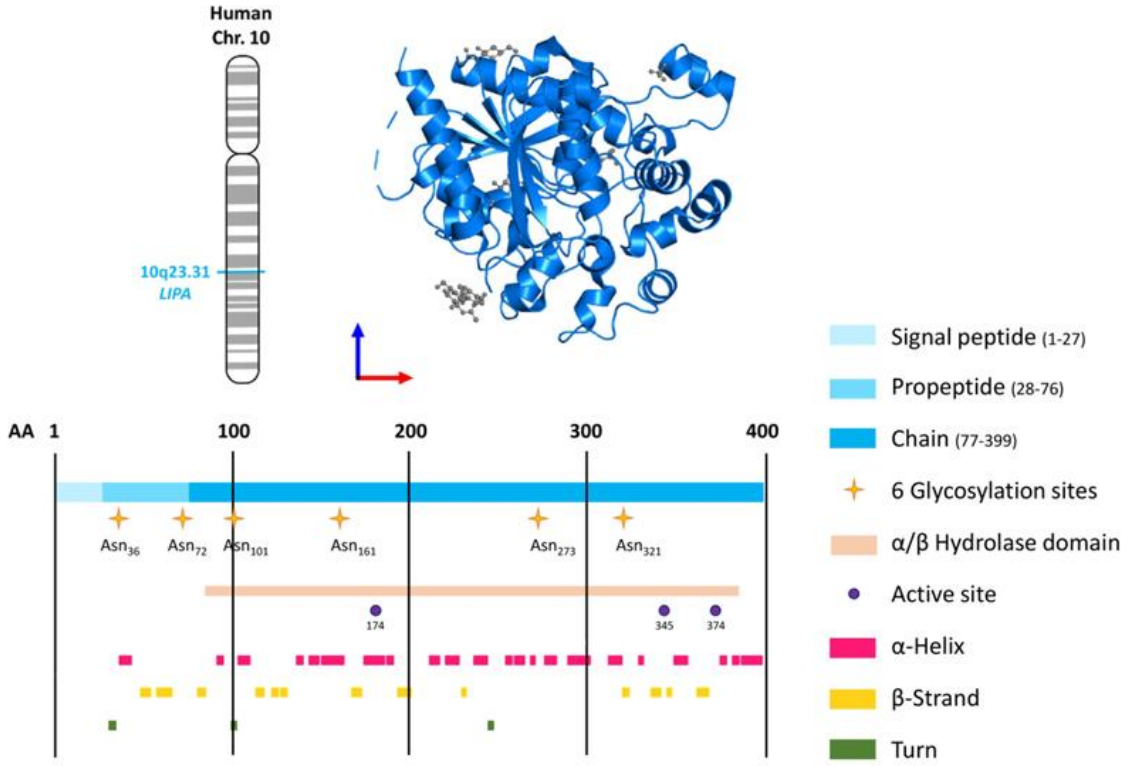

Figure 1. Chromosomal location of the human LIPA gene and structure of human LAL protein.(Korbelius et al. 2023) Structure of human lysosomal acid lipase (LAL).

Lysosomes catabolic machinery and export mechanisms are constantly active to prevent storage of any degradation products. LAL is mainly regulated by starvation at the transcriptional level. Sirtuin 1 deacetylates forkhead box protein O1 and peroxisome proliferator-activated receptor γ coactivator 1α in response to nutrient restriction upregulating directly LIPA transcription. It has also been reported that transcription factor EB (TFEB) regulates LIPA gene by mammalian Target of Rapamycin inhibition, leading to dephosphorylation and translocation of TFEB to the nucleus, resulting in an up regulation of LIPA gene (Dubland and Francis 2015). Moreover, LAL can be modified at post-transcriptional level at macrophages by oxidized or aggregated LDL due to the increased lysosomal pH (Heltianu et al. 2011).

FC and FA derived as hydrolytic products of LAL degradation, serve as energy sources, biosynthesis of cell membranes, precursor for oxysterol, hormones, bile acid and vitamin D. In the hepatocyte the internalization of LDL, (Figure 2, (A)) the source of TG and CE, together with lipid droplets are carried out by receptor-mediated lysosomal endocytosis and products released, free cholesterol (FC) and fatty acids (FA) degraded by LAL, are a critical regulator of overall lipidic homeostasis. In this aspect, the lysosomally-derived cholesterol pool has impact through inhibiting sterol regulatory element binding protein (SREBP) cleavage activating protein in the ER, regulating the new cholesterol synthesis and LDL receptor expression by the cell. Whereas the exact mechanism of lysosomal FA export remains unclear, lysosomal FC export occurs via Niemann–Pick disease type C 1 and 2 proteins (Korbelius et al. 2023). When FC levels in lysosomes are elevated, SREBP-2 downregulates the expression of LDL receptors, leading to a decreased uptake of

cholesterol into the cell. Additionally, the inhibition of hydroxymethylglutaryl-coenzyme A (HMG-CoA) reductase reduces cholesterol synthesis, while the activation of acyl-CoA-cholesterol acyltransferase (ACAT) enhances cholesterol esterification. This process serves as a protective mechanism to prevent the toxic effects of excess FC on cellular membranes. At the same time, intracellular fatty acid enrichment leads to the inhibition of phospholipid and triglyceride production via SREBP-1c-mediated down-regulation of fatty acid synthesis (Reiner et al. 2014). Instead, a reduced or absent activity of LAL, leads to an accumulation of CE and TG in lysosomes (Figure 2, (B)). The intracellular FC absence causes SREBP-mediated upregulation of *de novo* cholesterol production by HMG-CoA reductase and endocytosis of LDL receptors as well as very-low-density lipoprotein cholesterol (VLDL-C) augmented secretion and an increased synthesis of ApoB, resulting in an enhanced LDL-C production, an important contributor of hypercholesterolemia in LAL-D patients.

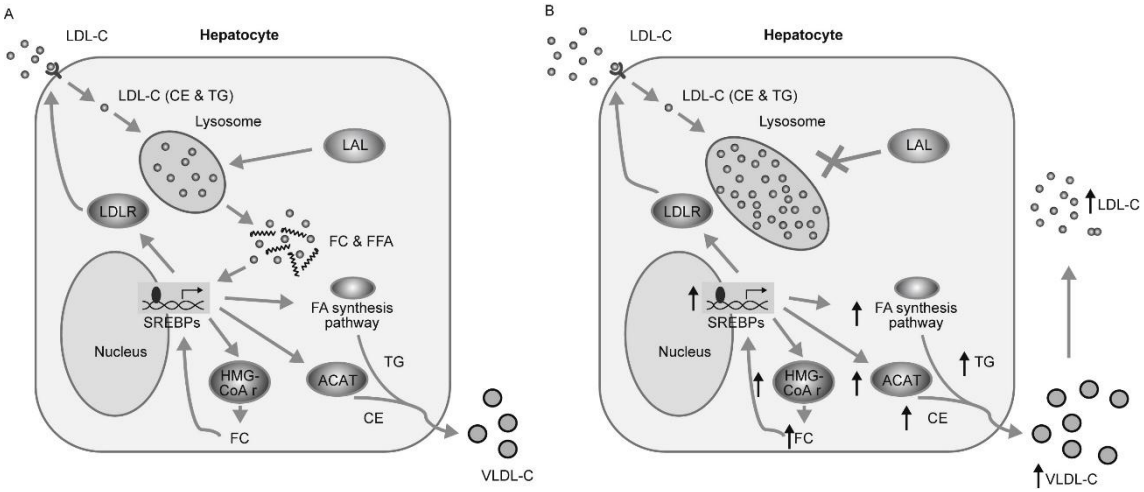

Figure 2. Cholesterol homeostasis in (A) healthy individuals and (B) LAL-D patients. (Reiner et al. 2014). Schematic view of cellular cholesterol homeostasis. LDL-C: low-density lipoprotein cholesterol; CE: cholesterol esters; TG: triglycerides; LAL: lysosomal acid lipase; FC: free cholesterol; FFA: free fatty acids; LDLR: low-density lipoprotein receptor; VLDL-C: very-low-density lipoprotein cholesterol.

Typical clinical manifestations in LAL-D patients are elevated TG and persistent dyslipidemia, which is caused by an elevated serum total cholesterol with high LDL-C and low HDL-C, due to the accumulation in plasma of ApoB-containing VLDL-C and LDL-C. However, the reduction of HDL-C is because of the elevated TG and decreased expression of adenosine triphosphate-binding cassette transporter A1, the responsible of HDL particle formation, by the reduced FC intracellular content and, consequently, a reduced activation of nuclear liver X-receptor as a promoter of ATP-binding cassette transporter gene.

3.1.2. Genetics

LAL-D is caused by mutations in the LIPA gene, located in chromosome 10q23.2-q23.3 which has 10 exons distributed in approximately 36 kb (Anderson et al. 1993), and is a disorder of cholesterol metabolism with an autosomal recessive mode of inheritance. Exists more than 600 variants reported, and among these, more than 100 variants are classified as pathogenic or likely pathogenic and are considered disease-causing variants

(around 25% of them associated with the infantile-onset phenotype, 50% with the later-onset phenotype and 25% with both) (de las Heras et al. 2024).
Both CESD and WD are caused by mutations in LIPA gene, and they are distinguished by the level of residual activity of mutant LAL, being in infantile-onset disease an absence of LAL activity. So far, various kinds of gene mutations causing WD and CESD have been identified. In general, nonsense mutations, deletions, and insertions in LIPA gene are associated with WD, although there are some exceptions (e.g., p.G245X). On the other hand, as to missense mutations, the phenotypes are heterogeneous; some of them cause WD, and the others CESD. (Saito et al. 2012).

The most common variant in LAL-D later-onset subtype is the nucleotide change c.894G>A, being the most prevalent mutation located in the canonical sequence for the splicing of pre-mRNA in the region exon 8-intron 8 (E8SJM, of exon 8 splice junction mutation) present in ~60% of patients with LAL-D of European origin (Camarena et al. 2017). According to a study performed in more than 15,000 *LIPA* alleles from healthy African American, Asian, Caucasian, Hispanic, and Ashkenazi Jewish individuals from New York and Dallas, the frequency of the c.894G>A allele was 1:1000 for the Asian population and approximately 1:300 for the Caucasian and Hispanic populations. Assuming that c.894G>A accounted for 60% of reported multi-ethnic later-onset LAL-D variants, the predicted prevalence of later-onset LAL-D is approximately 0.8 per 100,000 (Scott 2013). A novel variant, c.966+2T>G, was reveled in a study of 23 Spanish patients with LAL-D (13 with infantile-onset disease and 10 with later-onset disease) and accounted for 75% of the infantile-onset LAL-D alleles (Ruiz-Andrés et al. 2017).

3.1.3. Clinical Presentations

There are typical features that suggests a LAL-D diagnosis as elevated serum total cholesterol, elevated serum transaminases, liver fibrosis, cirrhosis and hepatomegaly. WD may be differentiated from CESD based in their clinical manifestations as well as in the LAL activity.

In the infantile-onset LAL-D patients, the symptoms begin during the first weeks or usually before the first month, although some abdominal distention in the affected infant may be evident immediately after birth (Aguisanda, Thorne, and Zheng 2017).
The main clinical manifestations of infantile-onset LAL-D include digestive disorders, such as malabsorption, steatorrhea, vomiting, and diarrhea, leading to malnourishment and failure to thrive, as well as persistent abdominal distension with hepatosplenomegaly (Table 1). The enlargement and calcification of the adrenal glands, which can be detected trough abdominal radiographs, is a key feature of WD that although is a ubiquitous pathological feature of WD, is not essential.
Hemophagocytic lymphohistocytosis (HLH) is common at diagnosis in patients with rapidly progressive infantile-onset LAL-D and is due to uncontrolled immune activation with an acute and rapidly progressive systemic inflammatory response. A biopsy of the small intestine can show infiltration of the lamina propria by foamy macrophages filled with CE and TG so, the liver, spleen, lymph nodes, and tonsils may also be enlarged due to accumulation of these lipids in lysosomes of infiltrating macrophages and other cells.

The accumulated lipids activate these macrophages, leading to their transformation into foam cells (Aguisanda, Thorne, and Zheng 2017). The activated macrophages produce proinflammatory cytokines, which contribute to systemic inflammation. If specific treatment is not initiated in a timely manner, the prognosis of patients with HLH and underlying infantile-onset LAL-D is severe or even fatal (de las Heras et al. 2024).

The biochemical susception includes biochemical abnormalities as elevated cholesterol total profile, low HDL-C, high ferritin values and fat-soluble vitamin deficiencies and, if infantile-onset co-occurs with HLH, the usual alterations observed are cytopenia, elevated ferritin, triglycerides, liver enzymes, bilirubin and lactate dehydrogenase, among others.

On the other side, patients with later-onset LAL-D or CESD can present with a remarkably diverse range of phenotypes, ranging from the onset of symptoms in infancy to a diagnosis as late as age 80 years (Pisciotta et al. 2009).
The clinical manifestations are highly variable because of the range of LAL activity level and may occur as early infancy or as late as the fifth and sixth decades of life. Given the nonspecific symptoms (Table 1) the disease is often misdiagnosed, being confused usually with Familiar Hypercholesterolemia, due the fact that the clinical suspicion arises from a biochemical altered profile. Hypertransaminemia and lipid profile alterations are the main biochemical characteristics of LAL-D (de las Heras et al. 2024), especially an elevated levels of serum total cholesterol, low HDL-C and elevated TG and transaminases, the latter of which can cause accelerated atherosclerosis and premature cardiovascular disease. Regarding the clinical features, these include hepatomegaly, splenomegaly, and hepatic steatosis which can develop fibrosis, cirrhosis, due the lipid deposition in the liver, and even hepatocarcinoma. Although CESD can be diagnosed both in children and adults, some symptoms may not appear until older age. CESD-related mortality is often due to liver failure and/or secondary accelerated atherosclerotic disease (Aguisanda, Thorne, and Zheng 2017).

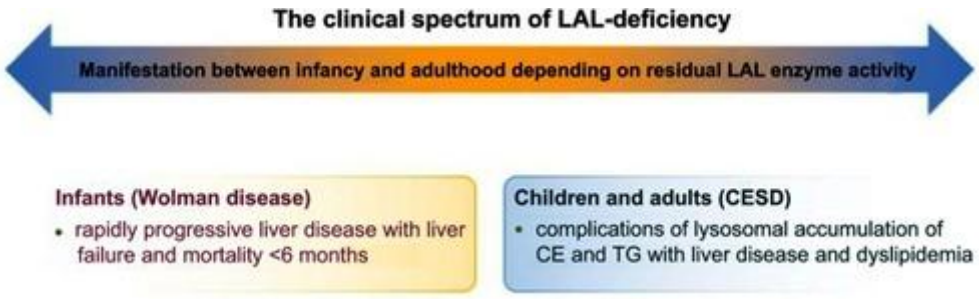

Figure 3. The clinical spectrum of LAL-D. (Strebinger et al. 2019). The clinical spectrum of LAL-deficiency ranges from severe variants with early death, previously referred to as Wolman disease, to milder variants manifesting during childhood or adulthood, known as CESD.

Table 1. Clinical manifestations in infantile and later-onset LAL-D patients.

Clinical Manifestations	Infantile-onset	Later-onset
Lipid Profile	Elevated LDL-C, TG. Reduced levels of HDL-C.	Elevated LDL-C, TG, serum total cholesterol. Reduced levels of HDL-C.
Liver Function	Elevated ALT + AST.	Elevated ALT + AST.
Hepatic Pathology	Yellow and greasy. Infiltration by lipid-filled Kupffer cells. Fibrosis.	Microvesicular steatosis of the hepatocytes. Cirrhosis. Infiltration by lipid-filled Kupffer cells and macrophages.
Splenic Pathology	Enlarged spleen.	Enlarged spleen.
Adrenal Pathology	Calcification of the adrenal glands.	Very rare calcification of the adrenal glands.
Intestinal Pathology	Massive CE and TG accumulation in the small intestine. Infiltration of the lamina propria by foamy macrophages.	CE accumulation, but to a much lesser degree than WD.
Biochemical Features	No functioning levels of LAL.	1-12% of functioning LAL relative to healthy patients.
Age of Onset	First few months of birth.	Childhood to Adulthood.
Life Expectancy	<1 year.	Patients live into adulthood.
Causes of Death	Malnutrition, malabsorption, liver failure.	Liver failure.

Adapted from (Aguisanda, Thorne, and Zheng 2017). Clinical and biochemical manifestations in infantile-onset and later-onset lysosomal acid lipase deficiency. LDL-C: low-density lipoprotein cholesterol; CE: cholesterol esters; TG: triglycerides; HDL-C: high-density lipoprotein cholesterol; LAL: lysosomal acid lipase; ALT: alanine amino transferase; AST: aspartate amino transferase; WD: Wolman disease

3.1.4. Diagnosis

A diagnosis of WD and CESD requires a determination of LAL activity level by a dried blood spot sample that enables indirect quantification. The determination is reliable, reproducible and can be carried out on diverse biological samples, although the most common is dry blood spot samples. LAL activity is determined in the presence of substrates, concretely 4-methylumbelliferone (4-MU), covalently modified with a fluorochrome which releases the fluorescent compound and can be quantified using fluorescence emission spectroscopy. Because 4-MU palmitate cleavage is not specific to LAL, a specific inhibitor is used to differentiate between general lipase activity and LAL activity (Aguisanda, Thorne, and Zheng 2017).

If the activity of the reference lysosomal enzyme is within the normal range, an analysis of the *LIPA* gene should be performed. Therefore, in such cases, it may be difficult to confirm the molecular diagnosis. In the case of a patient with suspected LAL-D and low

enzyme activity but inconclusive findings in the genetic study, the patient should be diagnosed with LAL-D (de las Heras et al. 2024).

Plasma biomarkers as liver enzymes and lipid profiles are routinely used in monitorization of LAL-D but a specific-disease diagnostic biomarker has not yet been identified. Still under investigation, LCN2 shows direct relation with liver injury. It is evidenced that LCN2 is massively overexpressed in the liver from patients with alcoholic hepatitis and its expression correlates with the degree of fibrosis and portal hypertension (Chen et al. 2020), therefore, extrapolation to fibrosis monitoring in LALD patients is sought.
Other parameters usually determined for the management of LAL-D are inflammation and oxidative stress biomarkers. Regarding inflammation, plasma chitotriosidase activity and CCL18/PARC activity, released by active macrophages, are often elevated, as it is CRPu. Other elevated biomarkers include cholesterol oxidation products or as named as oxysterols such as 7-Ketocholesterol and cholestane-3β,5α,6β-triol, which are markers of oxidative stress (Pajares et al. 2015). Inflammation biomarkers and oxysterols are also elevated in other lysosomal disorders or alterations in cholesterol metabolism, so they are not specific-disease diagnostic biomarkers and additional studies are required to diagnose LAL-D.

In parallel to biomarkers determination for the management of LAL-D, diagnostic tools as imaging, biopsy and histology are often used. In respect to imaging, abdominal x-ray, ultrasound and computed tomography are used to scan adrenal gland calcification in infantile-onset LAL-D as well as adrenal hypertrophy, hepatosplenomegaly and portal hypertension also characteristic in later-onset subtype. Quantification of hepatic fat is usually measured with nuclear magnetic resonance (NMR), however, transient elastography is now the most frequently used method given the limitations of liver biopsy, which is useful for diagnosis but given its invasive nature and the availability of other non-invasive methods it is often replaced. Even so, liver biopsy is the gold standard for the evaluation of liver involvement and assessment of fibrosis (Camarena et al. 2017), however, biopsies are carried out if there is clinically suspected liver disease.

Differential diagnosis is based on analysis of family and hereditary patter to distinct autosomal recessive and dominant disorders and is necessary due to the unspecific symptoms of LAL-D which could lead to confuse both infantile and later subtypes.

Differences between LAL-D and the most similar diseases are collected in Figure 4:

LAL-D	Familial Hypercholesterolemia	Non-Alcoholic Fatty Liver Disease
• Autosomal recessive • Biallelic *LIPA* mutation • Raised liver enzymes • High LDLc • Low HDLc • Variable increase in triglycerides • Hepatomegaly • Splenomegaly • Microvesicular steatosis (liver biopsy) • Variable degree of fibrosis usually present in pediatric population (liver biopsy)	• Autosomal dominant • Biallelic *LDLR*, *apoB*, *PCSK9*, *LDLRAP1*, *ABCG5*, and *ABCG8* mutations • Normal liver enzymes • High LDLc • Normal HDLc • No enlarged liver or spleen	• Genetic or environmental origin • Normal or raised liver enzymes • Usually normal LDLc and HDLc • No enlarged liver or spleen • Macrovesicular steatosis (liver biopsy) • Variable degree of fibrosis can be observed in adult population (liver biopsy)

Figure 4. (de las Heras et al. 2024). Differential diagnosis among LAL-D, familial hypercholesterolemia, and non-alcoholic fatty liver disease.

3.1.5. Therapeutic strategies

Therapeutic strategies depend on disease subtype, although the two pillars of treatment are a low-lipid diet and enzyme replacement therapy (ERT) with Sebelipase α.

WD is characterized by requiring immediate treatment due to the rapid progression, leading to death if treatment is not initiated in a timely manner. For that reason, diagnosis is as urgent as treatment. Once LAL-D is clinically suspected, the first step is the determination of LAL activity, and, if clinical/biochemical susception is very clear, it is indicated to initiate appropriate administrative procedures to start treatment as soon as diagnosis is established.
Regarding ERT, the treatment should start with once-weekly doses of Sebelipase α of 3 mg/kg at the beginning and increasing to 5 mg/kg. The results, based on two previous studies, revealed improvements in patients who survived the age, reduced levels of biomarkers of liver dysfunction and hepatosplenomegaly, and improvements in anemia and gastrointestinal symptoms. The development of significant neutralizing anti-drug antibodies (ADA) associated with an attenuated response to ERT was reported in three children with complete deletion of the *LIPA* gene; thus, patients with complete deletion of the *LIPA* gene may have a higher risk of developing a significant neutralizing ADA response (de las Heras et al. 2024).

According to the pharmacodynamics of Sebelipase α, the initiation of the therapy leads to the breakdown of accumulated lysosomal lipids, which initially causes elevations in LDL cholesterol and triglyceride levels during the first 2 to 4 weeks of treatment. Typically, these lipid levels then decline to below baseline values within 8 weeks. In patients with elevated alanine aminotransferase (ALT) at baseline (82 out of 84 in clinical trials), reductions in ALT are generally observed within 2 weeks of starting treatment.

Treatment interruption results in increases in LDL-c and ALT levels, as well as a decrease in HDL-c. The pharmacokinetic behavior of sebelipase alfa was found to be nonlinear, showing a more than proportional increase in drug exposure when the dose was increased from 1 to 3 mg/kg, as determined by non-compartmental analysis in 26 adult participants. There was no evidence of drug accumulation with weekly or biweekly dosing schedules. Based on a population pharmacokinetic model, parameters were estimated in 65 pediatric and adult patients who received intravenous KANUMA at a dose of 1 mg/kg during Week 22 (see Table 2). This group included 24 children aged 4–11 years, 23 adolescents aged 12–17, and 18 adults. The pharmacokinetic profiles observed in adolescents were comparable to those seen in adults. Additionally, the time to reach maximum concentration (Tmax) and the elimination half-life (T1/2) were consistent across all age groups (European Medicines Agency 2024).

Table 2. Mean (SD) Pharmacokinetics Parameters at Week 22 in Pediatric and Adult Patients Receiving 1 mg/kg Once Every Other Week.

Parameter	4-11 years old	12-17 years old	≥ 18 years old
	N=24	N=23	N=18
AUC (ng·hr/mL)	942 (388)	1454 (699)	1861 (599)
Cmax (ng/mL)	490 (205)	784 (480)	957 (303)
Tmax (hr)	1.3 (0.6)	1.1 (0.3)	1.3 (0.6)
CL (L/hr)	31.1 (7.1)	37.4 (12.4)	38.2 (12.5)
Vc (L)	3.6 (3.0)	5.4 (2.4)	5.3 (1.6)
T1/2 (min)	5.4 (4.3)	6.6 (3.7)	6.6 (3.7)

Adapted from (European Medicines Agency 2024).

HLH could be developed while ERT, then anti-inflammatory treatment may be needed. Regarding nutrition, it serves as management for LAL-D by low-lipid diet as a substrate reduction therapy. Infantile-onset subtype involves, due to the lipidic accumulation along the lamina propria, gut damage and malabsorption leading to, often, a protein intolerance and only tolerate elemental formulas. This formula must be based on minimal fat (the recommended intake of essential fatty acids and long-chain polyunsaturated fatty acids should be ensured), amino acids, and monosaccharides. Regarding proteins, as essential macronutrients, a minimum intake of 4 g/kg/day should be provided in the form of free amino acids. In addition to macronutrients, it is important to ensure an adequate supply of electrolytes, vitamins (fat-soluble and water-soluble), and liquids tailored to the age and needs of the individual patient. In this case, multivitamin, mineral, and trace element preparations can be used, as can oral rehydration solutions. Due to malabsorption and organomegaly, enteral feeding may initially be better tolerated through a nasogastric tube in small boluses or as a continuous infusion (de las Heras et al. 2024). Once gut damage has been restored after feeding with elemental formula for over 4-6 weeks, whole proteins could be gradually introduced. It is important to monitor the influence of factors such as organomegaly and ascites and also circulating molecules such as lipid-soluble vitamins, essential fatty acids and iron levels.

On later-onset LAL-D subtype, lowering-lipid diet is recommended as substrate reduction therapy during whole life. The recommended dosage of Sebelipase α is 1 mg/kg, administered as an intravenous infusion once every other week, with dose escalation to 3 mg/kg once every other week in cases of suboptimal response based on clinical and/or biochemical criteria (European Medicines Agency 2024). Results revealed that patients receiving ERT observed significant improvements in altered lipid profiles and atherogenic biomarker levels.

Lipid-lowering drugs may also play a role in the management of later-onset LAL-D subtype, although patients receiving ERT, the use of those drugs is not usually required. Ezetimibe is used in LAL-D patients by reducing the absorption of cholesterol in the intestine. Studies have shown that it also reduces liver volume, hepatic cholesterol concentrations and serum transaminases (Chuang et al. 2014). Another study concluded that statins, inhibitors of the rate-limiting enzyme of cholesterol biosynthesis, got worse liver pathology by creating a vicious circle that attenuates the circulating cholesterol load but exacerbates hepatic lipid deposition (Figure 5), remaining its use as controversial. Statin treatment inhibits de novo cholesterol synthesis through blocking the rate-limiting enzyme HMG-CoA reductase and the reduced cholesterol availability attenuates VLDL-C secretion and lowers circulating cholesterol levels. Decreased cellular cholesterol levels also lead to activation of SREBP2 and compensatory upregulation of rate-limiting enzyme HMG-CoA reductase to sustain cellular cholesterol homeostasis, but this is inhibited by statins. In addition, activation of SREBP2 results in increased LDL receptor synthesis, causing increased clearance of LDL from the circulation and uptake of LDL by the liver, then endocytosed LDL remains entrapped within the lysosome and exacerbates hepatic lipid deposition and liver disease in LAL-D (Korbelius et al. 2023).

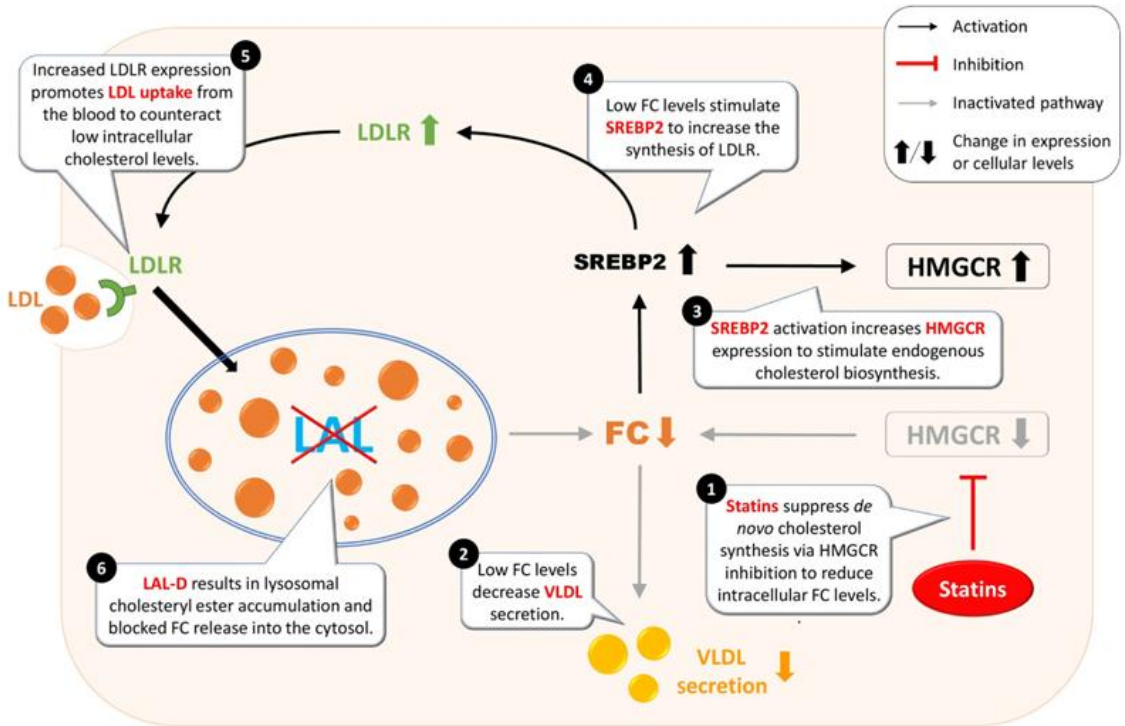

Figure 5. Potential problems of statin treatment in lysosomal acid lipase deficiency (LAL-D) patients. (Korbelius et al. 2023). LDLR: low-density lipoprotein receptor; LDL: low-density lipoprotein; VLDL: very-low density lipoprotein; LAL-D: lysosomal acid lipase deficiency; HMGCR: HMG-CoA reductase.

Recently, emerging treatments such as gene therapy have been under investigation and regarding LAL-D, a recent study has shown promising results for a single-treatment therapy using an adeno-associated virus in a preclinical model of Lipa-/- mice (Lam et al. 2024).

3.2. Atherosclerosis, cardiovascular disease and its relationship with LAL-D

LAL-D is caused by mutations in LIPA gene, causing decreased LAL activity and leading to, in CESD, an elevated LDL-C and low HDL-C and develop premature atherosclerosis, indicating the critical role LAL plays in cellular cholesterol and lipoprotein metabolism. (Dubland and Francis 2015).

Atherosclerosis is characterized biochemically by the accumulation of excess cholesterol in the artery wall, concretely LDL-C and other ApoB-containing lipoproteins that across an injured artery endothelium and get retained through charge-charge interaction with matrix proteoglycans in the subendothelial space. There, trapped lipoproteins suffer modifications such as oxidation or aggregation, converting them to ligands for scavenger receptors on intimal macrophages and smooth muscle cells (Figure 6). Receptors use the endocytic pathway for delivery of cargo to lysosomes, and then CE is hydrolyzed within lysosomes by LAL. FC released is transported out the lysosome by Niemann-Pick disease type C 1 and 2 transporters and re-esterificated by ACAT in the ER.

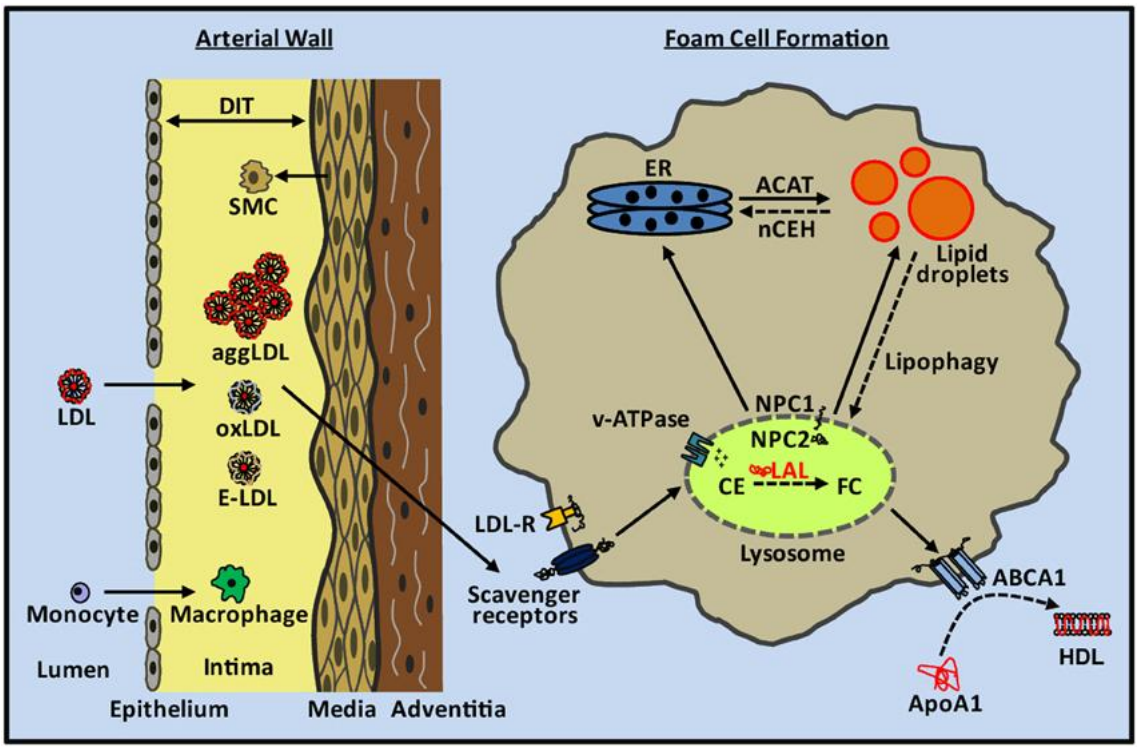

Figure 6. Cholesterol metabolism in atherosclerosis. (Dubland and Francis 2015). LDL: low-density lipoprotein; HDL: high-density lipoprotein.

Excessive uptake of modified lipoproteins leads to accumulation of CE there and giving a foamy appearance to them, forming cholesterol-overloaded foam cells. LAL has been implicated in LDL modification, and controversy aside, modified forms of LDL seem to

affect lysosomal function. LAL participates in modification of retained LDL, and its catalytic activity requires conditions that reduce pH. For that reason, macrophages can acidify the pericellular space through proton pumps and by secreting lactic acid (Buton et al. 1999). Excess of FC in the lysosomal membrane leads to loss of acidity as a result of inhibition of vacuolar H+-ATPase proton pumping activity and, consequently, loss of hydrolytic activity of LAL, and hence leads to lysosomal lipid droplet accumulation (Dubland and Francis 2015) (Figure 7).

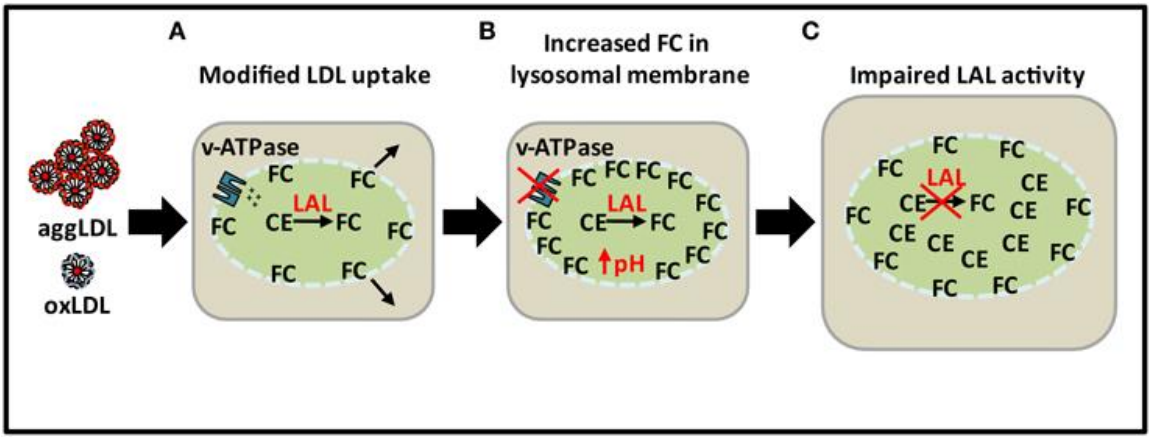

Figure 7. Loss of lysosomal function with excess lipid loading. (Dubland and Francis 2015). LDL: low-density lipoprotein; aggLDL: aggregated LDL; oxLDL: oxidated LDL; FC: free cholesterol; LAL: lysosomal acid lipase; CE: cholesterol esters.

The morphology of macrophages reflects their functional activation and microenvironment. Their high plasticity allows them to participate in a wide variety of processes. In the progression of atherosclerosis, we can find mainly two types of macrophages: On the one hand, elongated macrophages, which usually correspond to a more anti-inflammatory or reparative phenotype (frequently called M2), which participate in the resolution of inflammation and tissue remodeling and have less tendency to accumulate intracellular lipids. On the other hand, we can find foam cells, which are lipid-laden macrophages, characteristic of the initial and progressive phases of atherosclerosis, and their abundance indicates a greater uptake of modified lipoproteins and, therefore, a more propitious environment for the development and progression of atherosclerotic plaque.

Atherosclerosis can be associated to different parameters which can serve as surrogates of its level of progression. Monitoring IL-1β in atherosclerosis is useful because it reflects vascular inflammation and plaque activity, helping to assess cardiovascular risk and response to anti-inflammatory therapies. Elevated IL-1β levels are associated with increased plaque progression and adverse cardiovascular events (Ridker et al. 2017). In addition, PI3K/Akt signaling pathway activation can induce monocyte chemotaxis, macrophage migration, increased intracellular lipid accumulation, neovascularization, SMC proliferation and dysfunction in lesions, all of which are involved in plaque formation (Zhao et al. 2021). Additionally to those mentioned above, we can use the quantification of LRP1 (Low density lipoprotein receptor-related protein 1) to associate it to progression of atherosclerosis. LRP1 is the main receptor responsible for the uptake

of esterified cholesterol from aggregated LDL and hypercholesterolemia upregulates LRP1 expression in human coronary vascular smooth muscle cells and macrophages causing foam cell formation (Benitez Amaro et al. 2021). Also, E-Selectin, as an endothelial function biomarker and as an adhesion molecule, its expression is increased by cytokines causing leukocytes to bind to it, thus unraveling the early stages of atherosclerosis. It is for this reason that the increase in E-Selectin is related to the initiation of atherosclerotic processes indicating this progression (Prasad and Mishra 2022).

Regarding cardiovascular disease, it is related to atherosclerosis due to the lipidic accumulation in lamina intima. Patients with LAL-D demonstrate complications related to atherosclerotic cardiovascular disease, which are likely related to both the dyslipidemia, because of abnormal hepatic lipid metabolism, and the impairment of cholesterol efflux from lipid-containing LAL-deficient macrophages (Burton et al. 2015). Sebelipase α reduces LDL-C, LDL particle number, and Apo B, and increases HDL-C and Apo A1, suggesting an anti-atherogenic effect. It is unknown whether Sebelipase α, has additional effects on atherosclerosis risk outside of its modulation of lipid parameters, and larger and longer-term studies would be necessary to determine cardiovascular event rates (Besler, Blanchard, and Francis 2022).

4. HYPOTHESIS AND OBJECTIVES

LAL-D patients are at risk for accelerated atherosclerosis and premature cardiovascular disease due to persistent dyslipidemia and there are studies that demonstrate that Sebelipase α, the recombinant form of LAL, reduces LDL-C, LDL particle number, and ApoB, and increases HDL-C and ApoA, suggesting an enhancement of atherosclerotic profile. However, improvements aside from lipidic profile have not been studied yet.

Based on previous knowledge and studies, as well as aspects that remain to be explored, the following **hypothesis** is proposed for the project:

Administration of Sebelipase α, human recombinant LAL, in patients with LAL-D improves the atherosclerotic profile, beyond the lipid profile.

In order to test whether our hypothesis is correct, we will perform the project in reference to the following **objectives**:

1) Analyse of lipid and hepatic profile in a LAL-D patient (in ERT) and in a healthy control (without ERT) to support the relationship between LAL-D and atherosclerosis at three different times since the administration of Sebelipase α.
   1.1) Determination of: lipidic profile (LDL-C, HDL-C, TC, Non-HDL, TG), advanced lipid profile (Liposcale and Glycoscale Test) by NMR, hepatic profile (GGT, GPT) and uCRP as inflammatory biomarker.

2) Isolation and differentiation of macrophages from LAL-D patient (in ERT) and healthy control (without ERT) to evaluate its lipidic internalization and, consequently, its atherosclerotic progression at three different times since the administration of Sebelipase α.
   2.1) Isolation of VLDL+IDL and LDL from a control by ultracentrifugation.
   2.2) Isolation of monocytes-derived-macrophages from a LAL-D patient and a control.
   2.3) Incubation of VLDL+IDL and LDL with the monocytes-derived-macrophages.

3) Determination of atherosclerosis-related biomarkers in plasma and in macrophages from LAL-D patient (in ERT) and in healthy control (without ERT) to assess the progression of atherosclerosis at three different times since the administration of Sebelipase α.
   3.1) Determination in plasma of E-Selectin and Lipocalin-2 by ELISA.
   3.2) Analysis of the protein: LRP1 and IL-1β by Western Blot in cells.

5. METHODOLOGY

5.1. Study design and sample collection

Samples were collected from a patient with LAL-D with LIPA gene mutation c.894G>A, with a genetic diagnosis, and from a control individual without the mutation; the inclusion and exclusion criteria are collected in Table 3.
3 tubes of 10 ml (for monocyte extraction) and 1 tube of 6 ml (for plasma collection) of venous blood with EDTA as an anticoagulant have been extracted from the two individuals.
Collections have been performed at 3 different times within 15 days of ERT for LAL-D treatment (D1, D7 and D14). The 3 collection points will be established in the following way:

Figure 8. Collection timeline.

Inclusion criteria: Women of caucasian descent aged 24-25 years with a body mass index (BMI) within the normal range (22.3-22.5) was selected.

Exclusion criteria: Alterations in lipid profile or who if had received vaccination within the last three months was an exclusion criteria due to the potential impact on macrophage function.

Before starting with the methodology, a report to the drug research ethics committee was written and approved, giving step to the realization of the project under the administration of a drug, in this case Sebelipase α, the resolution is achieved in Annex I.

5.2. Human monocyte isolation from peripherical blood

The isolation of macrophages was carried out in a Bio2A laminar flow chamber under sterile conditions, using a total volume of 24 ml per sample (equivalent to 6 ml of blood for each of the 4 tubes used per sample). Ultimately, two Eppendorf tubes were obtained per sample, each containing the peripheral blood mononuclear cell (PBMC) layer suspended in 1 ml of RPMI medium (Gibco, USA).

The process began by adding 3 ml of Histopaque-1119 (Sigma-Aldrich, USA) to each 15 ml conical tube, followed by 3 ml of Histopaque-1077 (Sigma-Aldrich, USA), and finally 6 ml of blood on top of the Histopaque-1077 layer (overlayer). After centrifuging at 700 g for 30 minutes (brake off) (Figure 9), the plasma was aspirated and discarded, leaving a distance of 0.5 cm from the peripheral blood mononuclear cell (PBMC) layer. This layer

was then aspirated and transferred into 15 ml conical tubes to which 10 ml of RPMI medium was added.

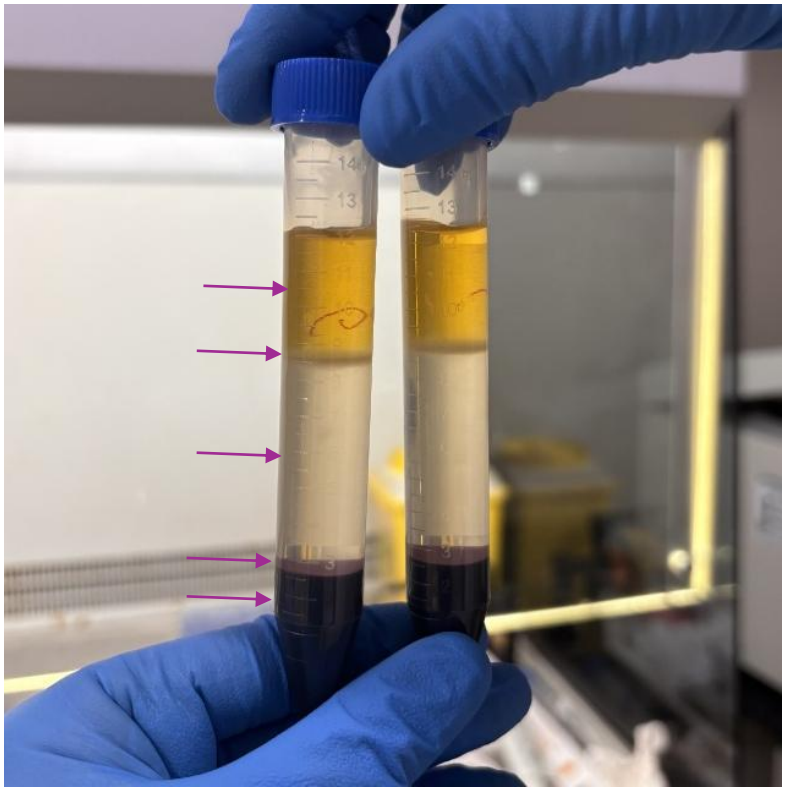

Figure 9. In order from top to bottom: Plasma, PBMC, Histopaque, granulocytes and red blood cells differentiation.

Following careful mixing and centrifugation at 200 g for 10 minutes, the washing procedure was carried out. The supernatant was discarded, and the cells were subsequently resuspended in 1 ml of RPMI medium. The washing process was repeated, and the pellet was resuspended and collected into two 2 ml tubes.

Cell counting was performed using a Neubauer chamber for both subjects. To prepare, 10 µl ml of resuspended cells, and 10 µl of Trypan Blue stain (Sigma-Aldrich, USA) were mixed in an Eppendorf tube, and a drop was placed in the Neubauer chamber for counting.

After collecting the PBMCs, each sample was divided into two criotubes (1ml/tub) and frozen in a Mr. Frosty™ Freezing Container at -80ºC containing isopropanol. The next day, samples were further frozen at -196ºC in a liquid nitrogen dewaruntil day 15, when all samples were processed. Prior to freezing, 10% of DMSO (Sigma-Aldrich, USA), concretely 100µl, was added as an antifreeze agent to prevent the formation of ice crystals during the freezing process (1ºC/hour). The protocol was repeated on samples from days 7 and 15.

Once all samples were processed, those from days 1, 7 and 15 were quickly defrosted at 37ºC. The samples were then spread and incubated in complete medium (RPMI+10FBS+1%P/S). After one hour, the medium was aspirated, and non-adherent cells (lymphocytes) were discarded. Finally, the remaining cells were washed twice with PBS and incubated with RPMI medium with and without VLDL+IDL and LDL.

5.3. VLDL and LDL isolation by ultracentrifugation

VLDL+IDL and LDL fractions were isolated from a pooled plasma sample obtained from 1 healthy donor (not including the LAL-D patient or healthy control) by sequential density gradient ultracentrifugation. We started the process with plasma samples (2 × 4 mL) that were thawed, and 3 mL from each tube were transferred into 5 mL ultracentrifuge tubes (Beckman Coulter, USA).

To isolate the VLDL+IDL fraction (density <1.006 g/mL), 2 mL of 1.006 g/mL density solution (Sigma-Aldrich, USA) was added to each tube. Samples were centrifuged at 37,000 rpm for 20 hours at 8°C using an Optima XPN-100 ultracentrifuge (Beckman Coulter, USA) equipped with a Kontron 50.2 rotor. The VLDL+IDL-containing supernatant was collected (1 mL per tube) and pooled. For LDL isolation, 1 mL of 1.023 g/mL density solution (Sigma-Aldrich, USA) was added to the remaining plasma in each tube, and the samples were centrifuged under the same conditions for an additional 20 hours. The LDL fraction was collected following centrifugation.

Both VLDL+IDL and LDL fractions were desalted by dialysis using 12–14 kDa molecular weight cut-off dialysis tubing (Medical Membranes Ltd, UK) against phosphate-buffered saline (PBS, Sigma-Aldrich, USA) at 4°C for 24 hours (2.5 L PBS per fraction). Dialysis tubing was pre-activated by heating in water at 100°C. After dialysis, samples were filtered using a 0.22 µm PVDF membrane (Millex, Ireland) under sterile conditions and stored at 4°C until use.

Protein concentration of the purified lipoprotein fractions was determined by the Lowry method. For this, an alkaline copper solution (A:C:B, 100:1:1, Sigma-Aldrich, USA) was prepared and protected from light. Solution D (Folin:H_2O, 1:1, Sigma-Aldrich, USA) was freshly prepared and kept in darkness. For each sample and standard (BSA), 10 µL was added to a 96-well plate (LDL samples were diluted 1:5; VLDL+IDL samples underwent delipidation prior to analysis). Then, 200 µL of alkaline copper solution was added (delipidated), mixed, and incubated for 10 minutes at room temperature in the dark. Next, 20 µL of solution D was added, mixed, and incubated for 30 minutes in darkness. For VLDL+IDL samples, 220 µL of chloroform (80–85%) was added, followed by vortexing and centrifugation at 2,000 rpm for 5 minutes. The aqueous (bluish) phase was transferred to the 96-well plate. Absorbance was measured at 650 nm using a Synergy spectrophotometer (BioTek Instruments):

Sample	Abs 650	µg/µl	Dilution	µg/µl	µg/µl
VLDL+IDL	0,219	0,795			**0,808**
	0,233	0,864			
	0,213	0,765			
Sample	**Abs 650**	**µg/µl**	**Dilution**	**µg/µl**	**µg/µl**
LDL	0,349	1,441	5	1,586	**7,928**
	0,378	1,586	5		
	0,407	1,730	5		

Table 3. VLDL and LDL concentrations.

5.4. Human macrophages incubation with VLDL+IDL and LDL

PBMCs were isolated from both a LAL-D patient and a healthy control at three different time points. Cryopreserved PBMC samples were thawed and washed twice with 10 mL of culture medium by centrifugation at 900 g for 10 minutes to remove residual DMSO. The resulting cell pellets were resuspended in culture medium and adjusted to a final volume of 13 mL per sample, aiming for a concentration of approximately 1×10^6 PBMCs per well.

For cell seeding, 1 mL of the cell suspension was added to each well of 6-well plates, and 0.5 mL to each well of 24-well plates. The cells were incubated at 37°C for 4 hours to allow adherence.

Subsequently, the culture medium was supplemented with either 100 µg/mL of a VLDL+IDL pool or 150 µg/mL of LDL pool (calculated from Table 12), according to the following experimental design (Figure 10). All conditions were incubated for an additional 24 hours at 37°C.

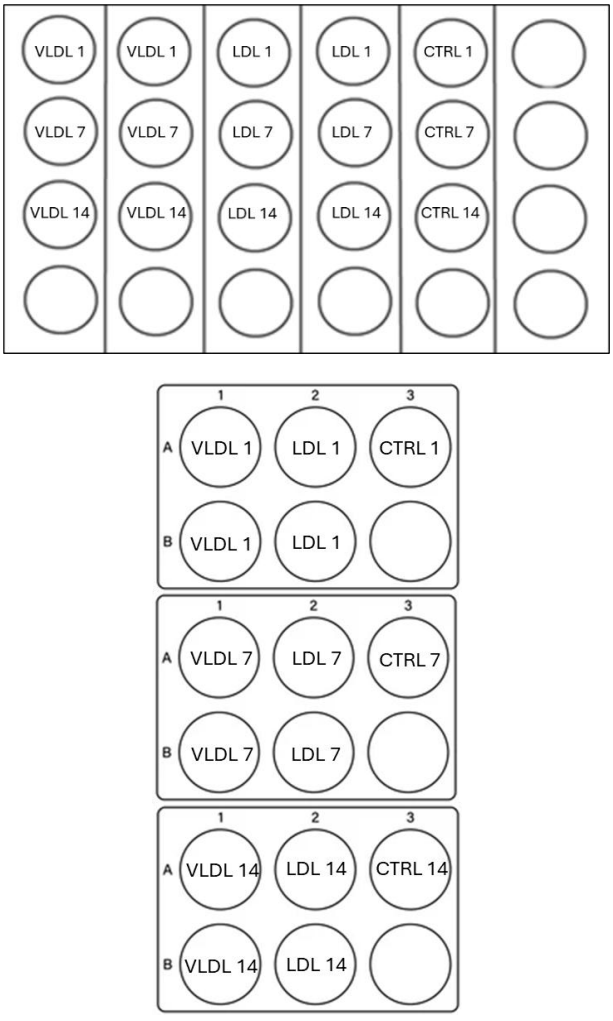

Figure 10. Plate design for incubation of samples from LAL-D patient and from healthy individual, with VLDL or LDL. Control well is without lipoprotein incubation. VLDL: very-low-density lipoprotein; LDL: low-density lipoprotein; CTRL: control (no lipoprotein).

After incubation time, it was the turn of incubation with Nile Red. A solution of Nile Red (Sigma-Aldrich, USA) (100ng/mL) was prepared using PBS, in order to visualize the intracellular lipids. Before Nile Red tinction and to make sure of this internalization, they were visualized under the microscope. The lipidic tinction was carried out to 24-well plates.

In the 6-well plates the total protein extraction was executed by Western Blot.

5.5. Cytotoxicity determination

To determine the cytotoxicity of the samples, the lactate dehydrogenase (Roche Diagnostics, Germany) cytotoxicity detection kit was used, which is a colorimetric assay for the quantification of cell death and lysis based on the measurement of lactate dehydrogenase (LDH) activity released from the cytosol of damaged cells in the supernatant.

We start with the thawing at room temperature of both samples and reagents. Once thawed, the catalyst solution was prepared in order to prepare the reaction mixture. In a 96-well plate we added 100 µl of sample in each well and 100 µl of reaction mixture, left to incubate for 30 minutes in the dark and proceeded to read at 490nm.

5.6.Macrophages Nile Red staining

Intracellular lipid drops from macrophages were visualized by Nile Red tinction. Nile red is a lipophilic fluorescent dye used primarily to selectively stain and visualize intracellular lipid droplets within cells. Its function relies on its strong fluorescence in hydrophobic environments, such as those provided by neutral lipids and lipid droplets, while it remains non-fluorescent in polar (aqueous) environments. This property allows Nile red to specifically highlight lipid-rich structures when observed under fluorescence microscopy or analyzed by flow cytometry.

This process was started with the incubation of the cells with 100 ng/ml of lipophilic fluorescent dye Nile Red (9-diethilamino-5H-benzo[α]phenoxazine-5-un) in PBS for 5 minutes at ambient temperature without fixation. The visualization was performed in an inverted microscope (Olympus IX71).

5.7.Western Blot from cellular extracts

Cells were lysed in RIPA buffer (0.1% SDS, 150 mM NaCl, 1% Nonidet P40, 50 mM Tris-HCl, 0.5% deoxycholate) with phosphatase and protease inhibitors (Roche Diagnostics, Germany).

Protein concentrations were determined using the Bradford assay kit (Bio-Rad). The iBlot® Dry Blotting system (Life Technologies, USA) was used to transfer 20 µg of total protein to nitrocellulose membranes after separation in 10% SDS-PAGE gels (Cell Signaling Technology, Inc.). Antibodies against LRP1, IL1B, and actin (Cell Signaling Technology, Inc.) were used. Membranes were incubated with HRP-conjugated

secondary antibodies (Dake, Denmark), and bands were visualized using ECL detection reagents (Amersham, USA).

Band intensities were analyzed with ImageJ software and normalized to total non-phosphorylated protein or Actin.

The relative levels of the forms of LRP1 and IL1B were quantified after normalisation to the total protein levels. All of the values were expressed in arbitrary units (AU).

5.8. Lipocalin-2 and E-Selectin quantification by ELISA

Lipocalin-2 and E-Selectin from the plasma of two individuals were quantified by ELISA, following instructions from commercial kits (Raybiotech, USA).

The sandwich ELISA is an immunoassay used to detect and quantify specific antigens in a sample (Figure 11), concretely we detected LCN2 and E-Selectin. It involves capturing the target antigen between two layers of antibodies: a capture antibody immobilized on a plate and a detection antibody linked to an enzyme, in this kit is HRP-Streptavidin. Upon adding the substrate (TMB in both cases), a measurable color change occurs, indicating the presence and concentration of the antigen, in this case the concentration and the color intensity are directly related.

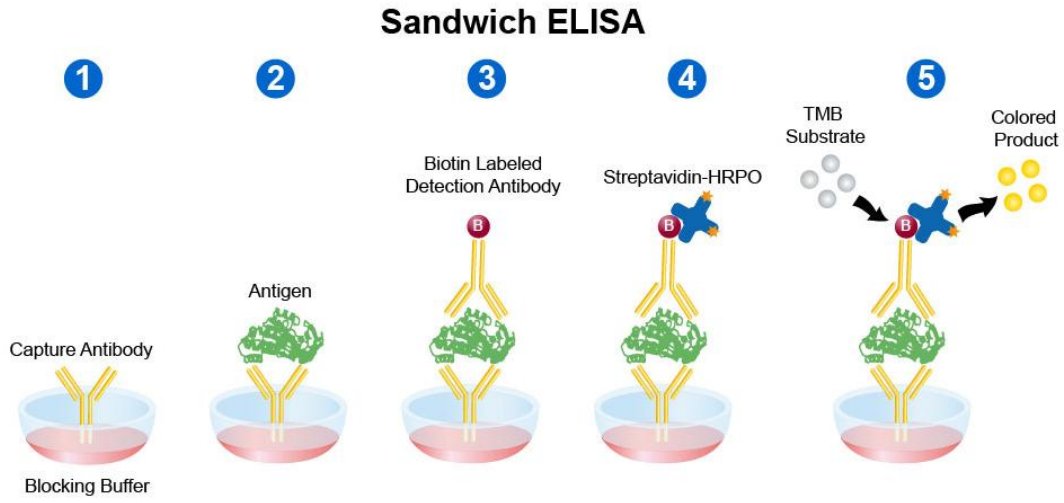

Figure 11. Sandwich. ELISA.

Regarding the protocols, the process started, for both quantifications, by defrosting plasma samples from two individuals. To be continued and, also for both quantifications, the standards were prepared following the protocol instructions (Figure 12) until fill 100 µl of sample by duplicate (previously diluted 100 and 50-fold) or standard (yellow cells) according to the following schemes and let them incubate for 2,5 hours in gentle agitation at room temperature:

1	2	3	4	5	6	7	8	9	10	11	12
BLANC	BLANC	AT1 (1:100)	AT3 (1:100)	AT2 (1:50)							
S1	S1	AT1 (1:100)	AT3 (1:100)	AT2 (1:50)							
S2	S2	GT1 (1:100)	GT3 (1:100)	GT2 (1:50)							
S3	S3	GT1 (1:100)	GT3 (1:100)	GT2 (1:50)							
S4	S4	AT2 (1:100)	AT1 (1:50)	AT3 (1:50)							
S5	S5	AT2 (1:100)	AT1 (1:50)	AT3 (1:50)							
S6	S6	GT2 (1:100)	GT1 (1:50)	GT3 (1:50)							
S7	S7	GT2 (1:100)	GT1 (1:50)	GT3 (1:50)							

Figure 12. Plate distribution for E-Selectin and LCN2 ELISAs.

In the E-Selectin protocol, the plasma dilution was with Assay Diluent A and, in contrast, in LCN2 protocol, with Assay Diluent B previously diluted 5-fold. After the first incubation was finished, we proceeded to wash and add 100 µl of the respective biotinylated antibodies to each well (previously diluted 80-fold with 1X Assay Diluent B for both kits) and left them to incubate for 1h hour under gentle agitation at room temperature. To be continued, the wash step was repeated and then was time to add 100 µl of prepared Streptavidin solution, previously diluted 600-fold for LCN2 kit and 900-fold for E-Selectin kit. Then, left them to incubate for 45 minutes at room temperature. After the wash step, 100 µl of TMB-One Step Substrate Reagent was added to each well and was incubated for 30 minutes at room temperature in the dark with gentle shaking. The last step was the addition of 50 µl of Stop Solution and read at 450nm immediately.

Samples concentration were extrapolated by standard curve.

5.9. Lipidic and hepatic profile and uCRP determination.

Plasmatic concentration of total cholesterol, TG, HDL-C, LDL-C, gammaGT, GPT and uCRP were determined by colorimetric and immunoturbidimetric methods, with Spinreact reagents adapted for the SPIN230 autoanalyzer (Spinreact, Spain).

The Spin230 autoanalyzer is a fully automated clinical chemistry analyzer designed for high-throughput sample processing. It features up to 80 sample positions and an auto-dilution system, ensuring precise measurements. The system uses disposable cuvettes to prevent contamination and maintains a reaction temperature of 37°C for optimal enzymatic activity. A halogen-tungsten lamp provides multiple wavelengths for accurate optical readings. Intelligent software manages calibration and quality control, making it efficient for laboratory diagnostics. Calibrators and samples were positioned following instructions and the results were obtained in its software ready to be exported.

5.10. Liposcale and Glycoscale determination by RMN

Size and number particles were determined from 9 lipoprotein fractions (small, medium and large VLDL+IDL, LDL, HDL) by NMR (Biofer Teslab, Spain). Plasmatic glycoprotein concentration (Glyc-A, Glyc-B and Glyc-F) was determined following the same analysis protocol of NMR, by an external company.

The Liposcale test includes advanced NMR-based molecular profiling of lipoproteins (Liposcale® test) and glycoproteins (Glycoscale® test) to aid in the characterization of cardiovascular risk from a lipid and inflammatory perspective simultaneously: Liposcale allows global characterization of lipoprotein composition, size and particle number;

Glycoscale allows characterization of inflammation biomarkers associated with the presence of glycated proteins, the production of which increases in systemic inflammation processes.

The arterial silhouette is a representation of 12 variables associated with cardiovascular risk, allowing for a quick and comprehensive assessment of the patient's lipid and inflammatory metabolism (beyond traditional parameters). These variables may change color to reflect different levels of risk: Red, yellow or green. The orange silhouette represents the patient's situation with respect to the values of a general population of 6,000 individuals (black circle). In the case of patients at high or very high cardiovascular risk, the dashed orange silhouette should be considered.

In order to contrast our hypothesis, Liposcale and Glycoscale results from a population of 89 individuals (considering our inclusion criteria) were provided to us by Biosfer TesLab.

6. RESULTS

In order to be able to interpret the following results, the characteristics of LAL-D patient and healthy individual, under which the study was carried out, are shown in Table 4:

Characteristics	LAL-D Patient	Healthy Individual
Age	24	25
Sex	Female	Female
BMI	22,5	22,3
Medication	-Sebelipase α -Ezetimiba	No

Table 4. Parameters to consider, LAL-D patient and healthy individual (control).

Lipidic and hepatic profile and uCRP determination

The lipid profile results of the LAL-D patient undergoing ERT and the healthy control were obtained with the aim of supporting existing literature, thereby demonstrating the relationship between ERT and the reduction of parameters that promote atherosclerosis. Each graph displays the trend of each parameter over time for both groups, with LAL-D patient data shown as blue circles and control data as light blue squares (Figure 13).

Across all five biochemical parameters shown in Figure 13 (Total Cholesterol, HDL-C, LDLc-C, TG, and Non-HDL), the LAL-D patient and healthy control show different trends over the 14-day treatment period. Health control data for most parameters remain relatively stable or show mild decreases during the treatment period. In panel **A)** LAL-D patient decreases by day 14; control remains stable. In panel **B)** Both remains slightly stable, with patient LAL-D data always remaining below control data. In panel **C)** LAL-D patient increases at day 7, then decreases; control is stable. In panel **D)** Both groups decrease over time, more markedly in the LAL-D patient. In panel **E)** LAL-D patient increases at day 7, then decreases; control remains stable.

Table 5 shows the results from the percentage decrease of lipid parameters of day one respect day fourteen.

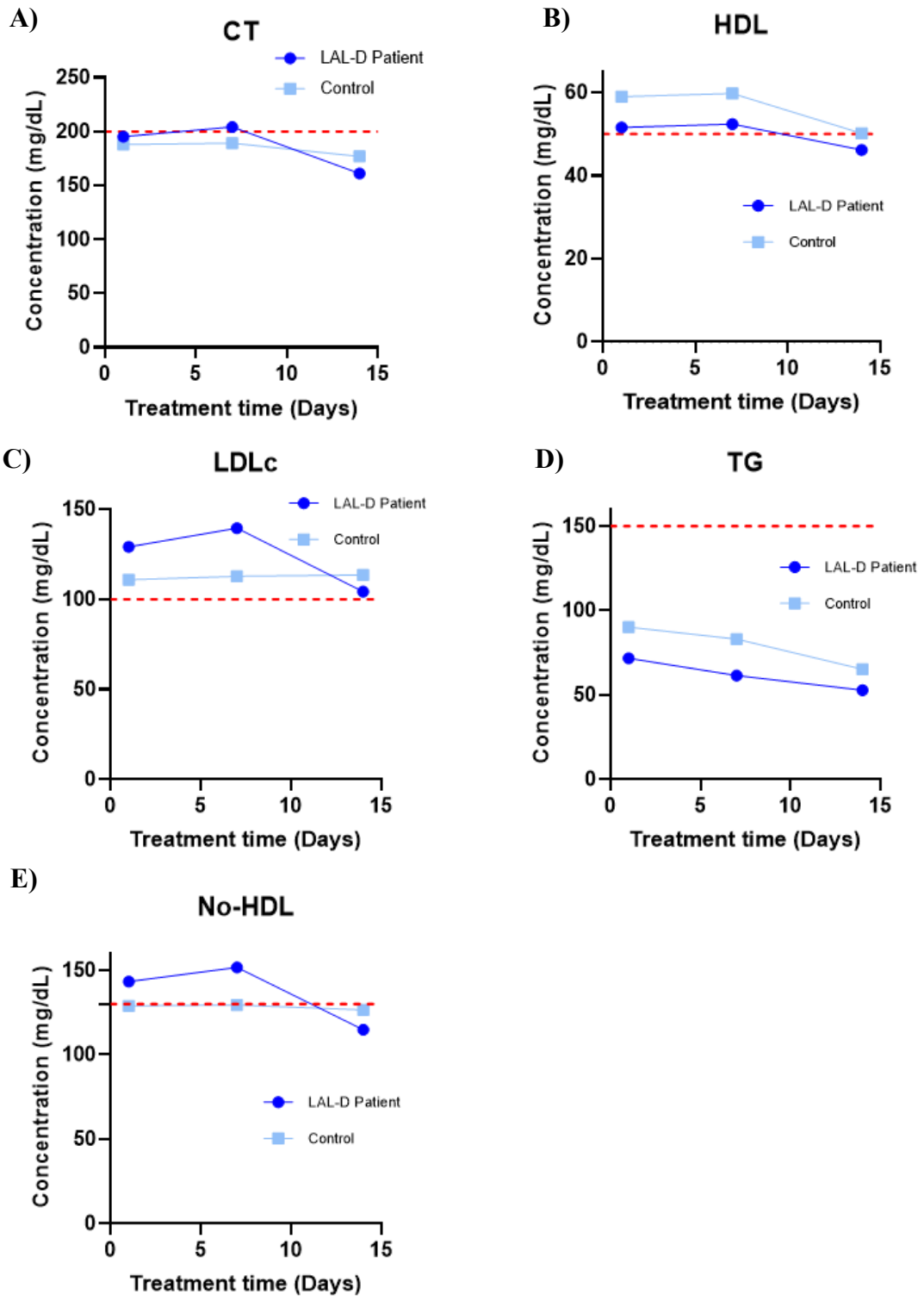

Figure 13. Concentration of various biochemical parameters measured in LAL-D patient and in a healthy control subject during a 15-day treatment period. These measurements were performed using a Spin230 autoanalyzer. ***A)*** *Total cholesterol concentration (mg/dL).* ***B)*** *HDL-C concentration (mg/dL).* ***C)*** *LDL-C calculated concentration by Friedewald formula (mg/dL).* ***D)*** *Triglycerides concentration (mg/dL).* ***E)*** *Non-HDL concentration. CT: Total Cholesterol; HDL: High-density lipoprotein; LDLc: Low-density lipoprotein Cholesterol; TG: Triglycerides; Non-HDL: Non high-density lipoprotein Cholesterol.*

Percentage decrease	LAL-D Patient	Healthy Individual
CT	-17,49%	-5,85%
HDL	-10,46%	-14,79%
LDLc	-17,5%	-5,85%
TG	-26,52%	-27,56%
Non-HDL	-19,85%	-1,78%

Table 5. Percentage decrease of biochemical parameters in reference to day one and day fourteen. CT: Total Cholesterol; HDL: High-density lipoprotein; LDLc: Low-density lipoprotein Cholesterol; TG: Triglycerides; Non-HDL: Non-high-density lipoprotein Cholesterol. LAL-D: Lysosomal Acis Lipase Deficiency.

In the case of hepatic biomarkers, represented in Figure 14, they fluctuate differently among themselves. On the other hand, uCRP concentration fluctuates more sharply in the LAL-D patient and according to the time of treatment. In panel **A)** LAL-D patient data remains stable during treatment-period. In panel **B)** LAL-D patient data performs inversely at control data. In panel **C)** LAL-D Patient remains upwards to control data.

The percentage decrease was also calculated in Table 6.

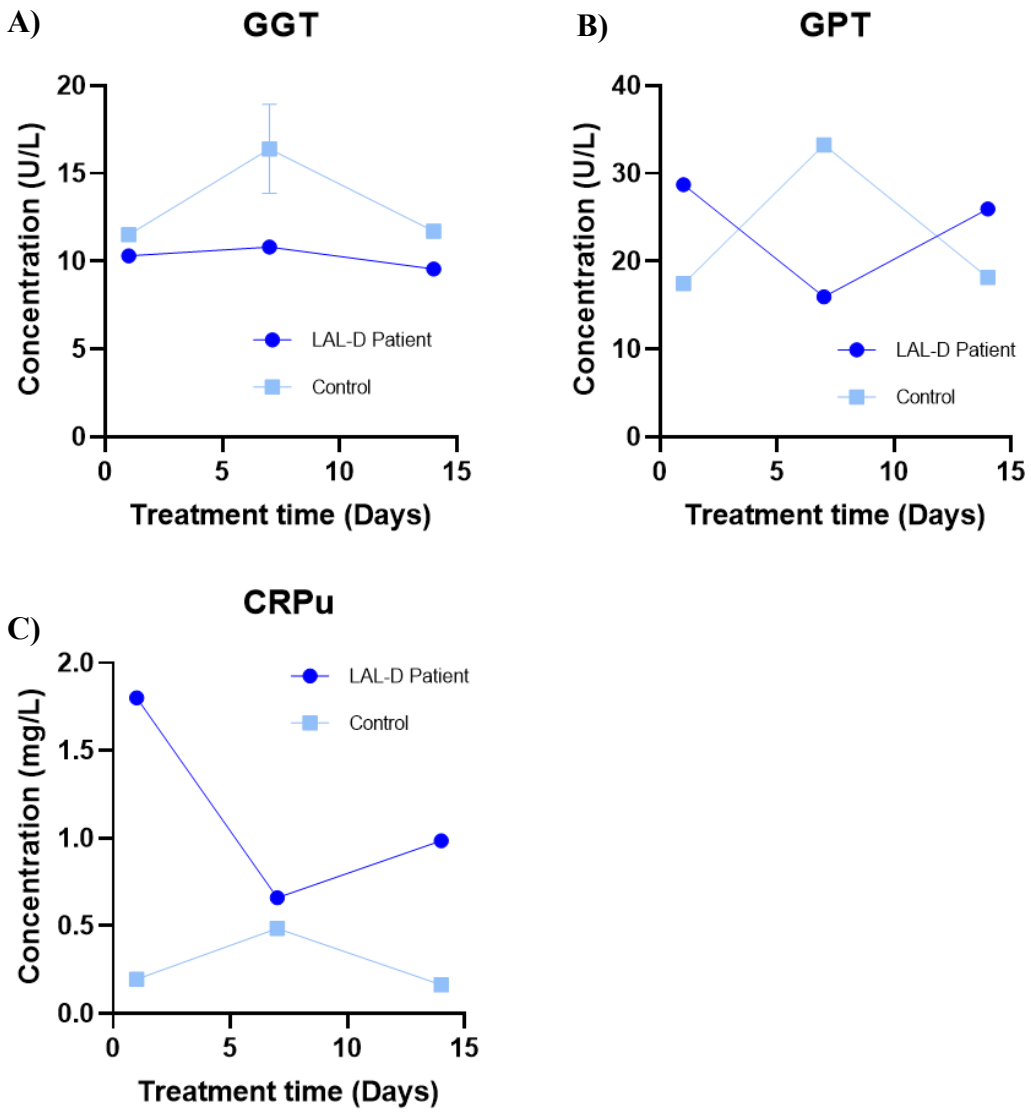

Figure 14. Concentration of hepatic and inflammation parameters measured in LAL-D patient and in a healthy control subject during a 15-day treatment period. These measurements were performed using a Spin230 autoanalyzer. ***A)*** *GGT concentration.* ***B)*** *GPT concentration.* ***C)*** *uPCR concentration. GGT: Gamma glutamyl transferase; GPT: Glutamic pyruvic transaminase; uPCR: ultra sensible C-Reactive protein.*

Percentage decrease	LAL-D Patient	Healthy Individual
GGT	-7,28%	+0,2%
GPT	-1,74%	+4,01%
CPRu	-45,28%	-15,38%

Table 6. Percentage decrease of biochemical parameters in reference of day 1 and day 14. LAL-D: Lysosomal Acis Lipase Deficiency. GGT: Gamma glutamyl transferase; GPT: Glutamic pyruvic transaminase; uPCR: ultra sensible C-Reactive protein.

Liposcale and Glycoscale determination by RMN

The next step, in line with the same objective, was the performance of the Liposcale+ Test on the LAL-D patient receiving ERT and the healthy individual at three different

time points following ERT administration, in order to more accurately differentiate or visualize cardiovascular risk.

In addition to Liposcale+ Test representation (Figure 15), the table in which these results were obtained can be found in Annex II.

Regarding the LAL-D patient and the healthy control in Figure 15, the orange silhouette is the one that has to be considered, because of not having hypertension or diabetes mellitus type II. As can be seen in Figure 15, the results of the LAL-D patient are slightly altered with respect to the healthy individual. In order to obtain solid conclusions, the results were compared with the mean (n=89), considering age, sex and BMI (Figure 17 and Table 6).

Comparing the results of the LAL-D patient under ERT with those of the healthy control in Figure 15, we observe that at all three time points, the representation of cardiovascular risk remains higher in the LAL-D patient. We can also note a decrease in this risk on day 14, coinciding with the lowest concentration peak of several risk-increasing parameters such as LDL-C or TG, among others.

On the other hand, regarding the population of 89 healthy individuals (Figure 16 and Table 7), we confirm that our selected healthy subject is suitable as a control, as their lipid parameters closely align with those of the broader healthy population. When comparing the results of the LAL-D patient under ERT to this reference group, the most notable differences are observed in the following variables: VLDL-C and Glyc-A: lower in the LAL-D patient; LDL-C and LDL-P: higher in the LAL-D patient.

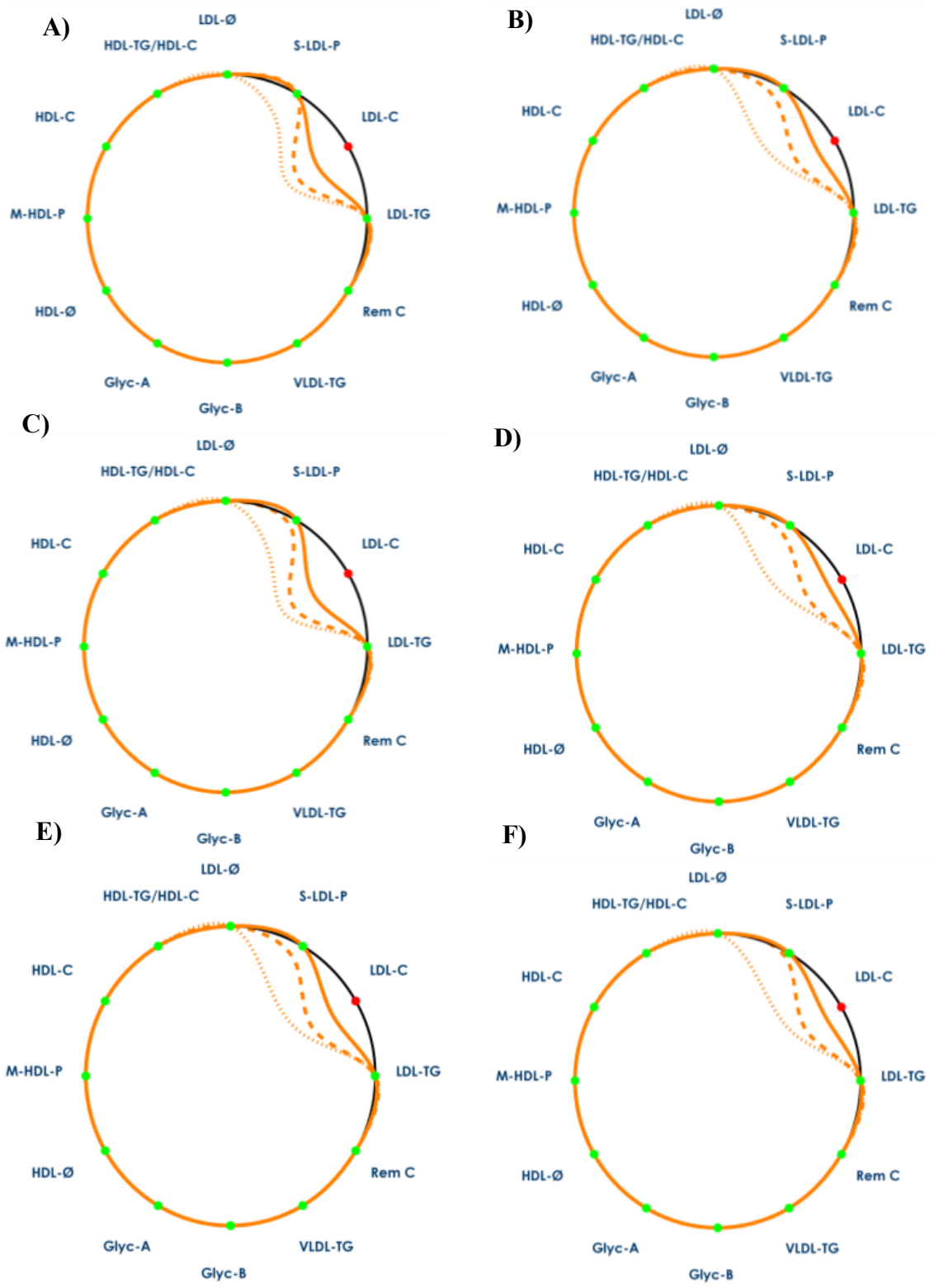

Figure 15. Liposcale+ Test results plots showing advanced lipoprotein profile analysis. Panels on the left ***(A, C, E)*** *correspond to the LAL-D patient, while panels on the right* ***(B, D, F)*** *correspond to a healthy control. Each row corresponds to the different treatment-day to LAL-D patient (Row 1=Day 1; Row 2=Day 7; Row 3=Day 14). Each plot displays multiple lipoprotein and glycoprotein parameters, including HDL-C, LDL-C, LDL-TG, VLDL-TG, Gyc-A, B, and C, distributed around the circumference. The orange lines indicate the measured values for each parameter, with green dots marking reference points. These visualizations allow for a direct comparison of the lipoprotein distribution and profile between the LAL-D patient and the healthy control across the three different treatment times. LAL-D: Lysosomal Acid Lipase Deficiency.*

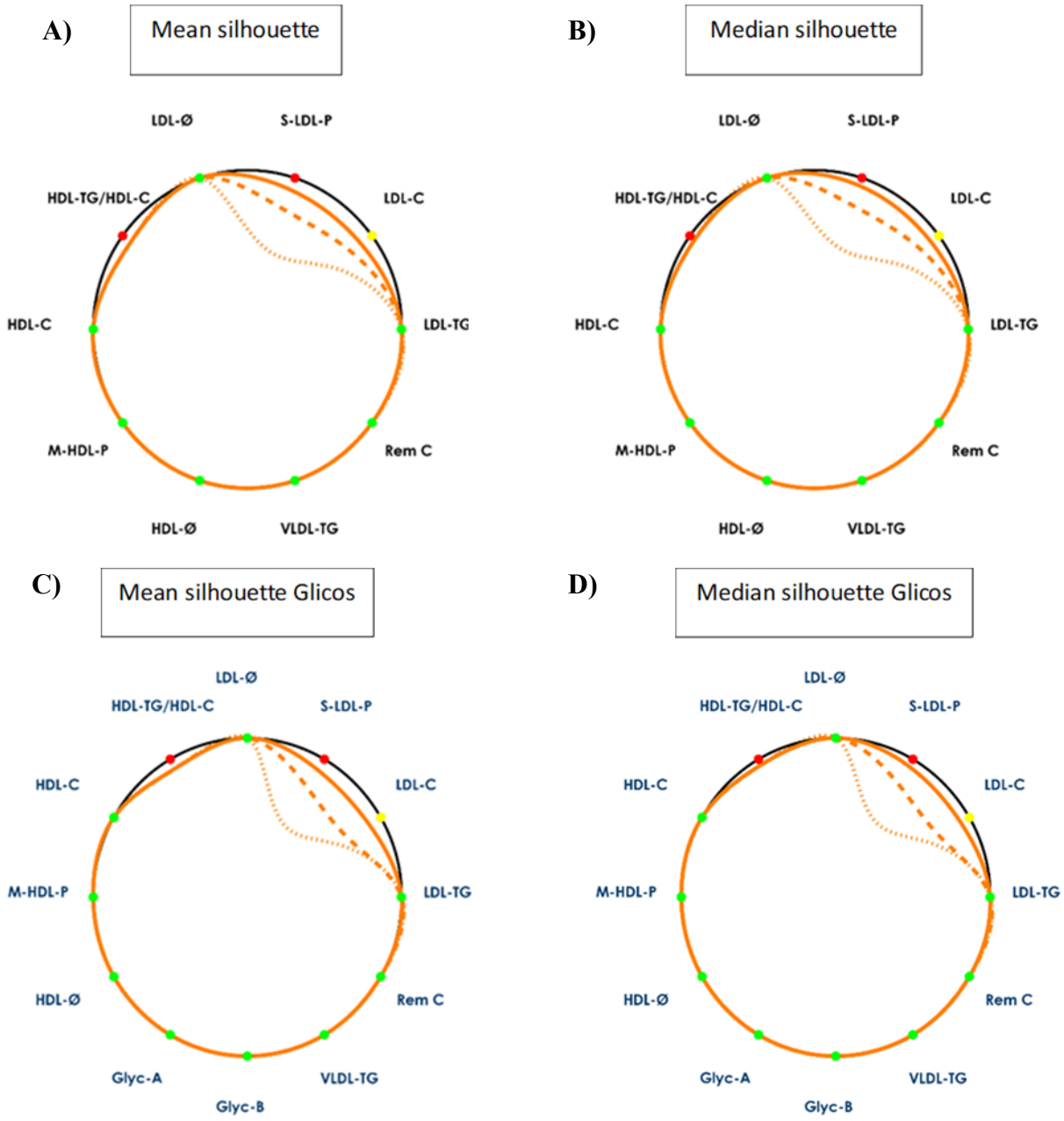

Figure 16. Liposcale+ Test in n=89 population, considering the same inclusion criteria (Sex, Age, BMI). ***A)*** *Mean silhouette.* ***B)*** *Median silhouette.* ***C)*** *Mean silhouette of Glycoproteins.* ***D)*** *Median silhouette of Glycoproteins.*

	[ALL]	LAL-D (day 1)	Control (day 1)	LAL-D (day 7)	Control (day 7)	LAL-D (day 14)	Control (day 14)
	N=89	*N=1*	*N=1*	*N=1*	*N=1*	*N=1*	*N=1*
Edad	26.0 [23.0;27.0]	24	25	24	25	24	25
SEX: Women	89 (100%)	1	1	1	1	1	1
IMC	22.6 [21.8;23.5]	22.5	22.3	22.5	22.3	22.5	22.3
HTA140:							
No	86 (96.6%)	1	1	1	1	1	1
Yes	3 (3.37%)	0	0	0	0	0	0
DM2: No	89 (100%)	1	1	1	1	1	1
VLDLC (mg/dL)	9.45 [6.17;13.8]	5.73	9.22	4.11	9.94	4.25	6.74
IDLC (mg/dL)	7.32 [4.97;10.1]	8.79	4.99	8.59	5.27	6.69	6.05
LDLC (mg/dL)	112 [101;130]	147.41	125.87	152.13	119.28	134.06	123.71
HDLC (mg/dL)	57.2 [50.0;65.5]	62.11	64.69	63.29	64.07	65.24	58.40
TotalC (mg/dL)	189 [169;213]	224.03	204.77	228.12	198.56	210.50	194.90
VLDLTG (mg/dL)	40.1 [33.1;52.2]	37.89	55.76	32.82	50.33	32.11	40.88
IDLTG (mg/dL)	8.63 [6.95;10.7]	8.47	6.53	7.99	7.40	7.69	7.24
LDLTG (mg/dL)	11.9 [8.88;14.8]	15.89	10.61	15.49	10.09	12.78	10.51
HDLTG (mg/dL)	15.3 [11.6;19.6]	7.96	7.66	6.64	5.45	8.79	6.02
TotalTG (mg/dL)	78.1 [61.1;98.5]	70.20	80.57	62.93	73.26	61,37	64.66
VLDLP (nmol/L)	29.8 [24.5;40.0]	25.46	37.38	22.02	33.35	22.57	26.37
LargeVLDLP (nmol/L)	0.89 [0.69;1.16]	0.68	1.04	0.66	0.86	0.60	0.74
MediumVLDLP (nmol/L)	2.71 [1.58;4.28]	3.31	4.62	2.44	5.57	1.86	4.54
SmallVLDLP (nmol/L)	26.3 [21.9;35.4]	21.47	31.72	18.92	26.91	20.10	21.10
LDLP (nmol/L)	1119 [1007;1304]	1315.13	1170.88	1377.65	1123.53	1248.95	1130.99
LargeLDLP (nmol/L)	165 [144;184]	263.31	221.39	253.79	201.83	228.53	229.0
MediumLDLP (nmol/L)	282 [216;408]	508.75	337.78	531.82	322.18	401.89	327.38
SmallLDLP (nmol/L)	661 [612;733]	543.75	611.72	592.04	599.52	618.72	574.61
HDLP (nmol/L)	29.9 [26.5;33.5]	25.13	26.75	25.42	27.43	27.22	24.13
LargeHDLP (nmol/L)	0.24 [0.22;0.27]	0.34	0.29	0.33	0.26	0.30	0.27
MediumHDLP (nmol/L)	9.38 [8.80;10.7]	12.54	12.49	12.31	10.86	12.80	11.06
SmallHDLP (nmol/L)	20.1 [17.6;22.5]	12.25	13.97	12.78	16.31	14.12	12.80
VLDLZ (nm)	42.0 [41.6;42.2]	42.39	42.35	42.29	42.67	42.0	42.75
LDLZ (nm)	21.0 (0.33)	21.77	21.32	21.63	21.23	21.39	21.44
HDLZ (nm)	8.24 (0.07)	8.47	8.41	8.44	8.32	8.42	8.40
Glyc-B (µmol/L)	320 [296;362]	275.69	280.69	279.85	338.40	268.26	294.07
Glyc-F (µmol/L)	195 [176;216]	185.62	198.12	181.10	162.29	147.45	163.21
Glyc-A (µmol/L)	618 [564;693]	543.34	602.57	504.76	633.04	481.54	547.69
H/W Glyc-B	4.02 [3.72;4.55]	3,47	3,53	3.52	4.25	3.37	3.70
H/W Glyc-A	14.7 [13.2;16.3]	14.18	14,73	13.53	15.92	12.52	14.38

Table 7. Summary table of population of 89, LAL-D patient and control from three different time points, considering BMI, age and sex. HTA: hypertension arterial; DM2: type 2 diabetes; VLDL: very-low-density lipoprotein; LDL: low-density lipoprotein; HDL: high-density lipoprotein; TG: triglycerides; C: cholesterol; P: particle; Z: size.

Human monocyte isolation from peripherical blood

To continue, we carried out macrophage differentiation with the aim of assessing their behavior in response to ERT in the LAL-D patient at three different times from the administration by being incubated with different lipoproteins and determinate the role of this treatment in atherosclerosis progression

Before LDL and VLDL incubation, macrophage differentiation was visualized using the inverted microscopy. Macrophages were observed to be adherent to the bottom surface of the culture plate, which resulted in a darker appearance attributable to their focal plane within the microscopic field. In contrast, erythrocytes that were not completely removed during the washing steps appeared lighter and more refractile.

After incubation for 24h with a pool of VLDL (150 µg/mL) and LDL (100 µg/mL), lipid internalization by macrophages was confirmed using bright-field inverted microscopy. This process is consistent with established mechanisms by which macrophages internalize lipids and accumulate intracellular lipid droplets, a phenomenon central to foam cell formation and atherogenesis.

Cytotoxicity determination

Before continuing with the results obtained from macrophage differentiation, we show below the graph with the cytotoxicity, that was measured from the LDH concentration, by absorbance signal, to determine the validity of the results obtained in macrophages. This concentration is used since LDH is found intracellularly in a physiological manner, so elevated LDH signals would indicate possible cell death.

After VLDL+IDL and LDL incubation, it was not toxic for cells, as we can observe in Figure 17, an average absorbance was obtained among all the samples (incubated and non-incubated), resulting in cell viability in both subjects and all samples.

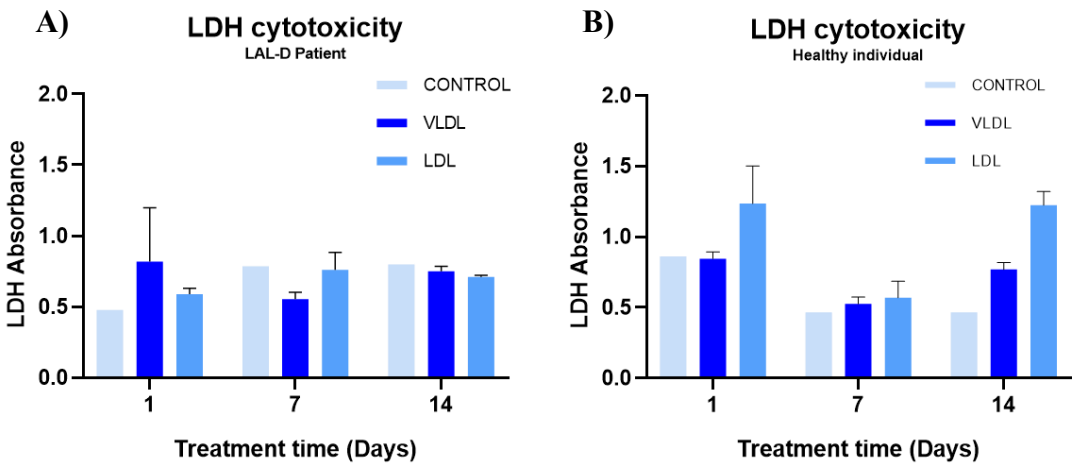

*Figure 17. Cytotoxicity measured in LDH absorbance of LAL-D patient (**A**) and of healthy individual (**B**) at three different times and in three different conditions: incubated with VLDL (150 µg/mL), LDL (100 µg/mL) or control (no lipoprotein). LDH: Lactate dehydrogenase; LAL-D: Lysosomal Acid Lipase deficiency; VLDL: Very-low density lipoprotein; LDL: Low-density lipoprotein*

Macrophages incubated with VLDL+IDL and LDL

Images acquired from 6-well plates were primarily intended to document the morphological features associated with macrophage differentiation. In contrast, the 24-well plates were specifically utilized for the visualization and assessment of lipid internalization by these macrophages. This methodological distinction allowed for optimized spatial resolution and comparative analysis of cellular phenotypes under varying experimental conditions.

With respect to the results obtained from the 24-well plate, and employing a different imaging approach (specifically, capturing images using a mobile phone camera directly from inverted microscopy) lipid droplets internalized within macrophages exhibiting an ovoid morphology can be visualized more distinctly. Distinct morphological characteristics of macrophages derived from a LAL-D Patient can be observed in in this set of experiments and the results are presented as a comparative analysis between macrophages derived from a LAL-D patient and those from a healthy control (Figures 18, 19, 20):

Across all three time points (days 1, 7, and 14), macrophages derived from the LAL-D patient (left columns) there appears to be a progressive and marked accumulation of intracellular lipid droplets, particularly following incubation with VLDL, as evidenced by the predominance of rounded, foam cell-like morphology. At baseline (no lipoprotein), these cells display a relatively homogeneous and slightly elongated appearance, but upon exposure to especially VLDL, there is a substantial increase in both the number and size of lipid droplets, with most cells adopting a rounded phenotype indicative of significant lipid uptake and storage. This condition, with the VLDL incubation, consistently shows the greatest degree of lipid accumulation and foam cell transformation. This morphological trend remains consistent across all three evaluated time points post-ERT, suggesting a stable response to the respective lipoprotein stimuli.

In contrast, macrophages from the healthy control (right columns) maintain a predominantly elongated and spindle-shaped morphology, with features described for M2-polarized macrophages, throughout all conditions and time points. Although elongated cells are more prevalent, lipid internalization is also observed in macrophages incubated with VLDL, as evidenced by the presence of intracellular lipid droplets. The overall cellular morphology remains largely unaffected, with no significant development of the foam cell phenotype.

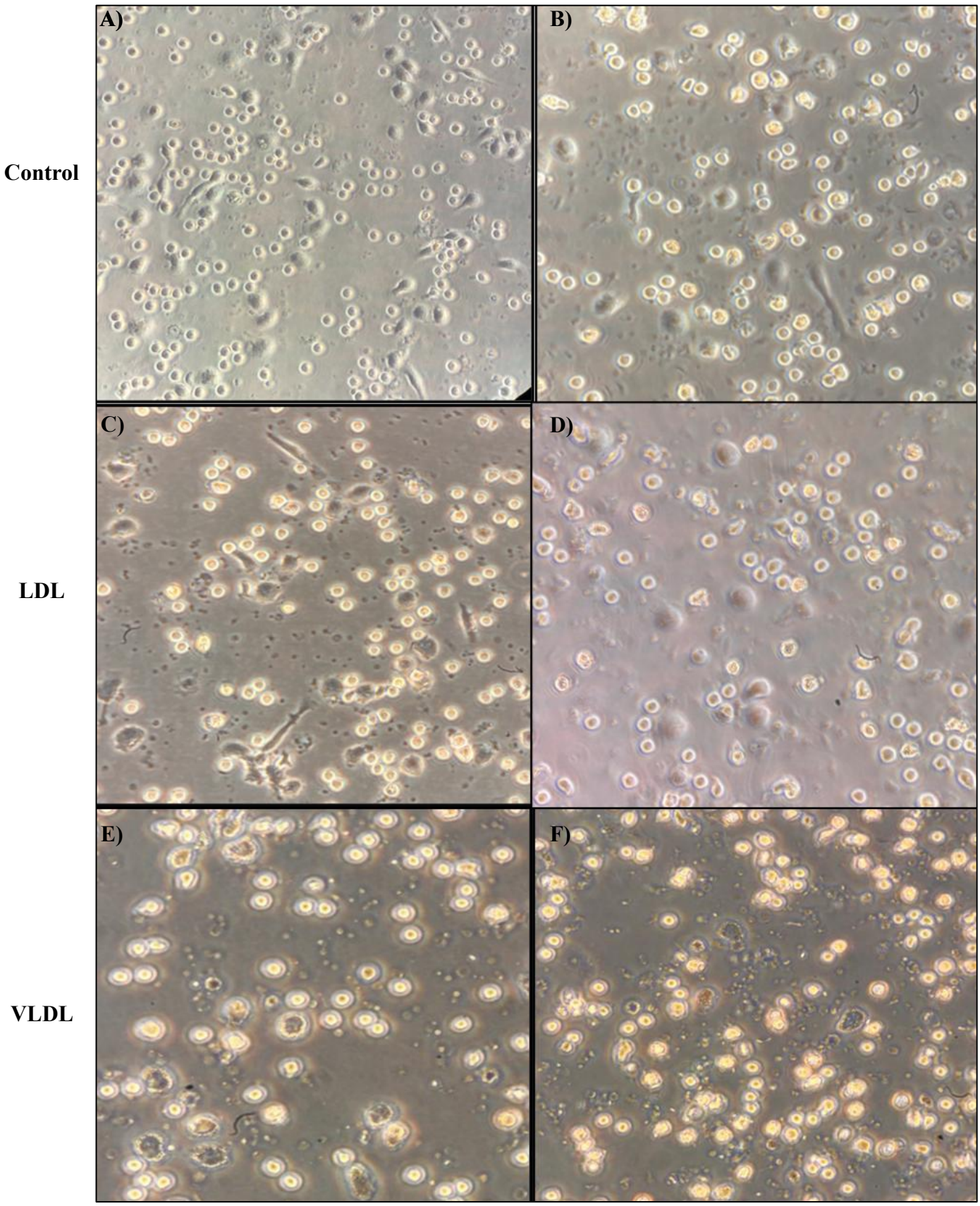

*Figure 18. Macrophages lipidic internalization from LAL-D (left) patient and healthy individual (right), both from **day one** visualized at x200. Panels **A** and **B** represents macrophages without lipoprotein incubation. Panels **C** and **D** represents incubation with LDL (100 µg/mL). Panels **E** and **F** represents incubation with VLDL (150 µg/mL).*

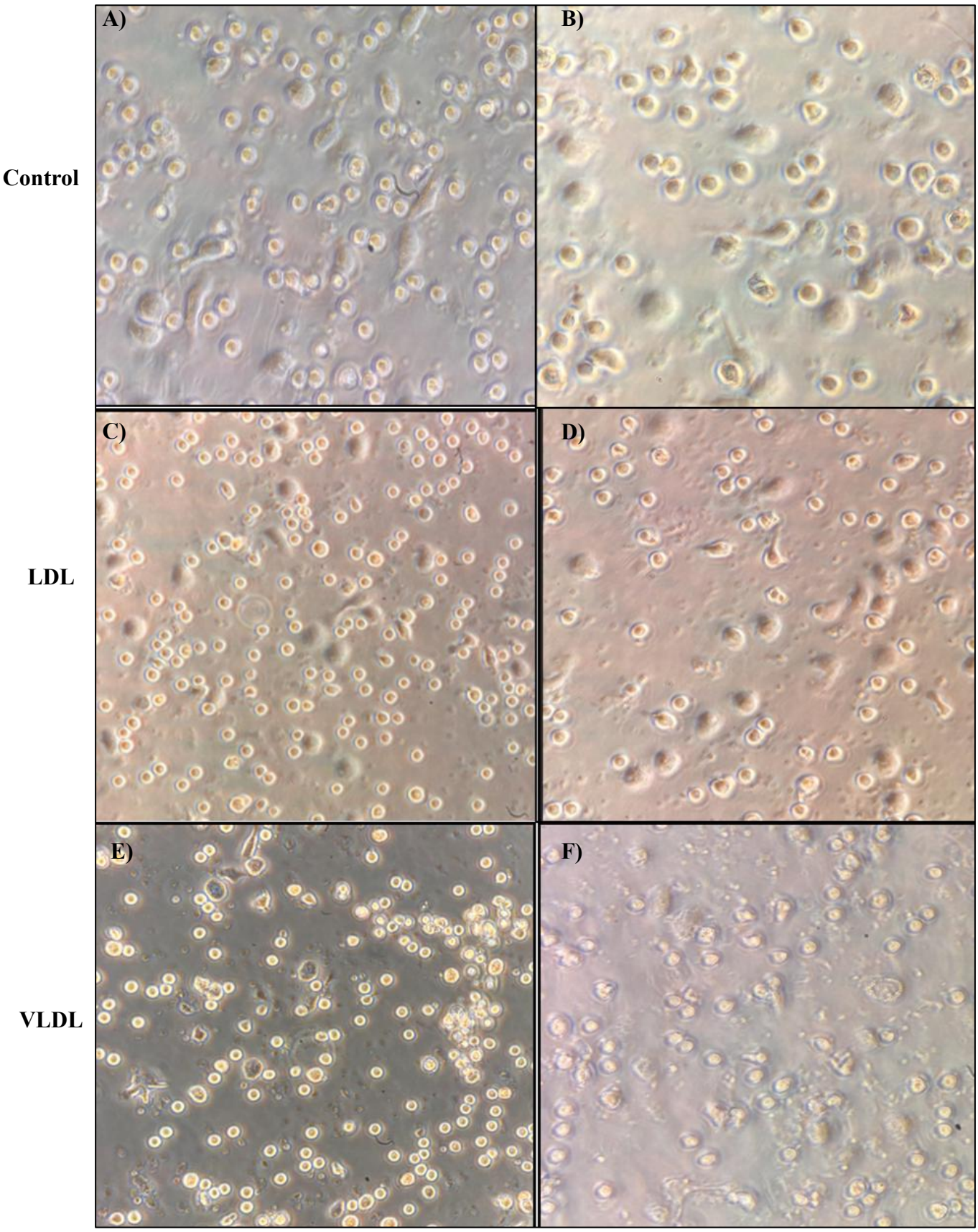

*Figure 19. Macrophages lipidic internalization from (left) LAL-D patient and (right) healthy individual, both from **day seven** visualized at x200. Panels **A** and **B** represents macrophages without lipoprotein incubation. Panels **C** and **D** represents incubation with LDL (100 µg/mL). Panels **E** and **F** represents incubation with VLDL (150 µg/mL).*

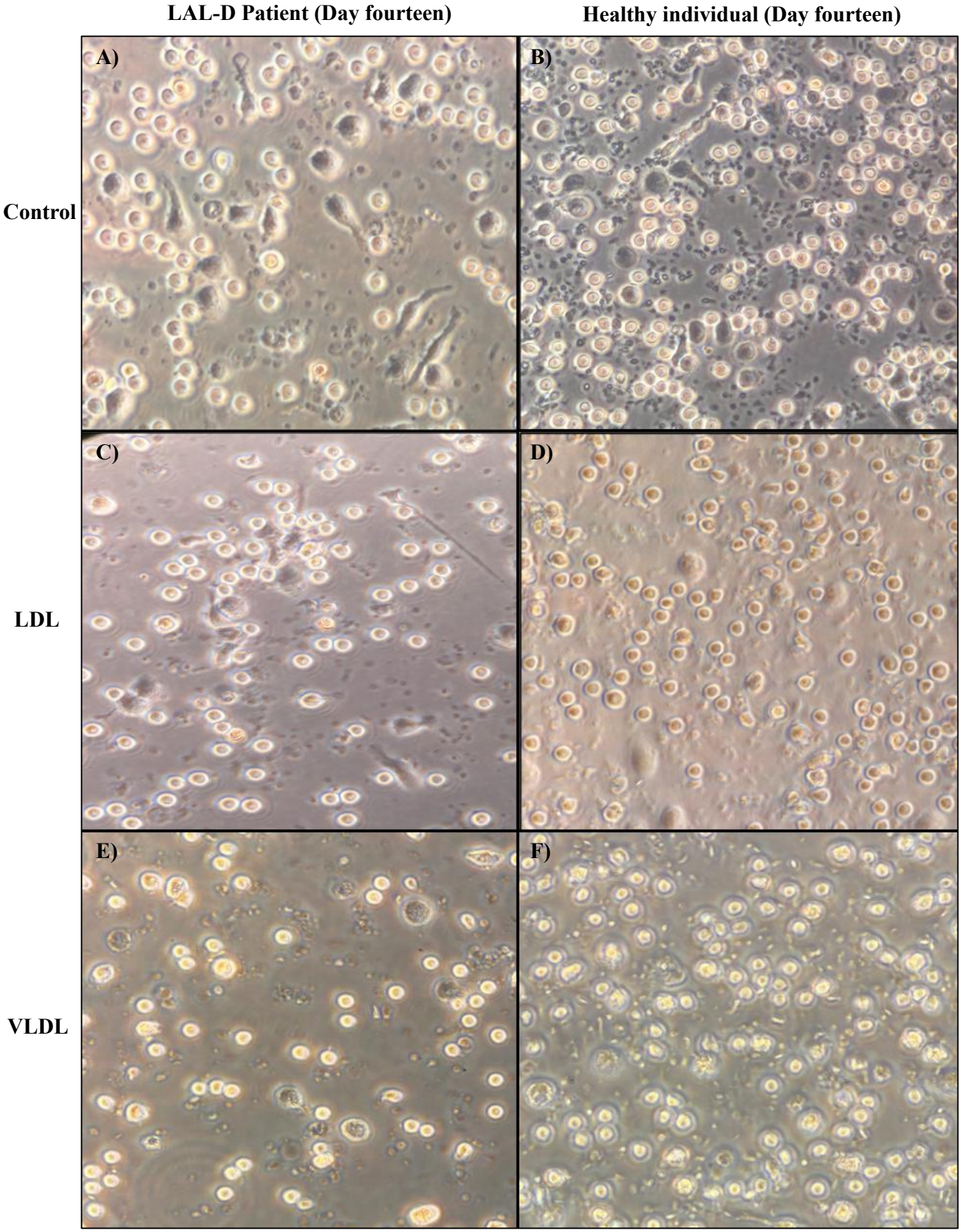

*Figure 20. Macrophages lipidic internalization from (left) LAL-D patient and (right) healthy individual, both from **day fourteen** visualized at x200. Panels **A** and **B** represents macrophages without lipoprotein incubation. Panels **C** and **D** represents incubation with LDL (100 µg/mL). Panels **E** and **F** represents incubation with VLDL (150 µg/mL).*

Nile Red, a selective fluorescent dye utilized for the detection and visualization of intracellular lipid droplets, was applied to the samples and incubated for 5 minutes. Following incubation, fluorescence was assessed using an inverted fluorescence microscope. The resulting observations are shown in Figure 21:

Across all three time points (days 1, 7, and 14 post-ERT), macrophages derived from the LAL-D patient (columns 1, 3 and 5) consistently exhibit low levels of Nile Red fluorescence, indicating minimal intracellular lipid accumulation. In the absence of lipoprotein incubation (top rows), fluorescence is barely detectable. Upon incubation with LDL (middle rows), there is only a slight increase in the presence of lipid droplets, which remain sparse and dimly fluorescent. After VLDL incubation (bottom rows), a modest increase in both the number and intensity of fluorescent lipid droplets is observed, particularly at day 7, but overall, the signal remains substantially lower than that seen in healthy controls.

In contrast, macrophages from the healthy control (columns 2, 4 and 6) demonstrate a markedly higher intensity of Nile Red fluorescence at all time points and under all incubation conditions. Without lipoprotein incubation (top rows), some baseline fluorescence is already evident. Following LDL incubation (middle rows), there is a clear increase in the number and brightness of intracellular lipid droplets. This effect is even more pronounced after VLDL incubation (bottom rows), where numerous, brightly fluorescent lipid droplets are observed, especially at later time points. These results indicate a robust capacity for lipid internalization and storage in healthy macrophages, which is further enhanced by exposure to lipoproteins, particularly VLDL.

As demonstrated by the fluorescence imaging in Figure 21, quantitative analysis revealed significantly higher fluorescence intensity in macrophages derived from the healthy control, with the greatest values observed following VLDL incubation, indicating robust lipid internalization. In contrast, fluorescence quantification in macrophages from the LAL-D patient showed markedly lower values overall. Notably, while VLDL-induced fluorescence was detectable in these samples, there was a clear trend toward decreased lipid internalization over time.

After the visualization in the inverted microscope, we proceeded with the quantification of this Nile Red fluorescence by ImageJ. Through pixels quantification, measured in raw integrated density and we will obtain a clearer and more general idea of the lipid internalization of macrophages at different times, as it is represented in Figure 22.

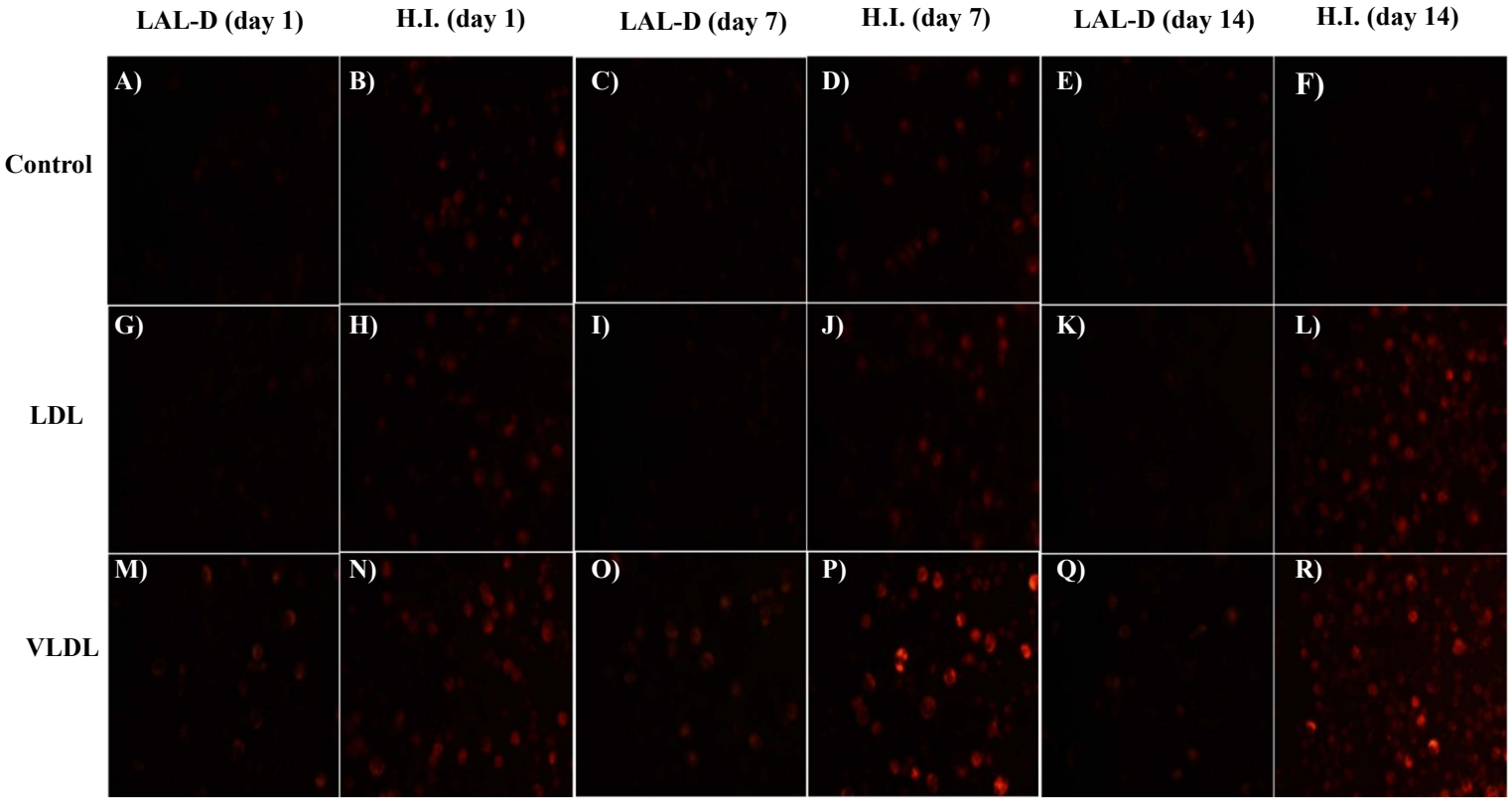

*Figure 21. Nile Red fluorescence staining of intracellular lipid droplets in macrophages from a LAL-D patient in ERT and a healthy control from **day one, seven and fourteen.** Representative fluorescence microscopy images are shown for macrophages derived from a LAL-D patient receiving ERT (**A, C, E, G, I, K, M, O, Q**) and from a healthy control (**B, D, F, H, J, L, N, P, R**). Rows correspond to different lipoprotein incubation: Control (**A, B, C, D, E, F**), LDL (100 µg/mL) (**G, H, I, J, K, L**), and VLDL (150 µg/mL) (**M, N, O, P, Q, R**). Nile Red staining highlights intracellular lipid droplets, with increased fluorescence intensity indicating greater lipid accumulation. LAL-D: Lysosomal Acid Lipase Deficiency; H.I.: Healthy Individual; LDL: Low-density lipoprotein; VLDL: Very low-density lipoprotein.*

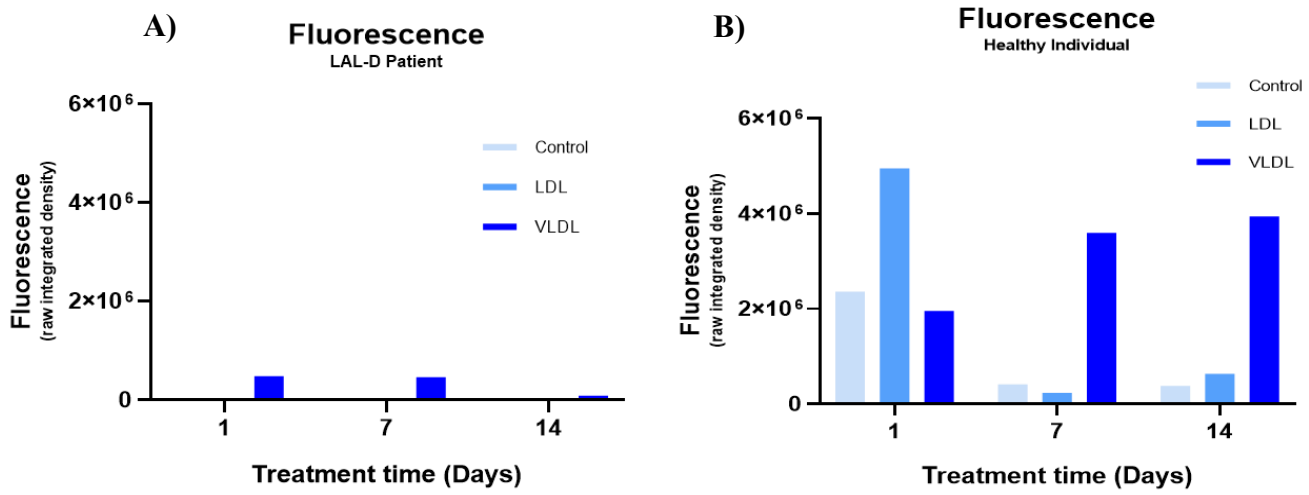

Figure 22. Fluorescence measured in Raw Integrated Density, from LAL-D patient (A) and healthy individual (B). LAL-D: Lysosomal Acid Lipase Deficiency. LDL: Low-density lipoprotein; VLDL: Very low-density lipoprotein.

Lipocalin-2 and E-Selectin quantification by ELISA

Finally, to address the third objective, we will perform ELISA and Western Blot techniques to assess, in both plasma and macrophage extracts, biomarkers associated with atherosclerosis. This will allow us to determine whether the treatment may influence the dynamics of these biomarkers depending on the time elapsed since its administration.

LCN2 and E-Selectin were measured in plasma to assess the effect of ERT in LAL-D patient: to monitor the atherosclerotic progression (E-Selectin) and liver injury (LCN2). Both biomarkers were quantified using sandwich ELISA techniques that allow for sensitive detection of target proteins. The measurements were taken at specific time points during the 15-day treatment period and by duplicate, with concentrations reported in ng/mL.

E-Selectin and LCN2 concentration are represented in Figure 23. E-Selectin levels, shown in panel **A** remains substantially higher in LAL-D patients than in control subjects throughout the entire treatment period. In contrast to E-Selectin, LCN2 concentrations in panel **B** are consistently lower in LAL-D patients compared to control subjects across all time points. The largest difference in LCN2 concentration appears on days 7 and 14 of treatment.

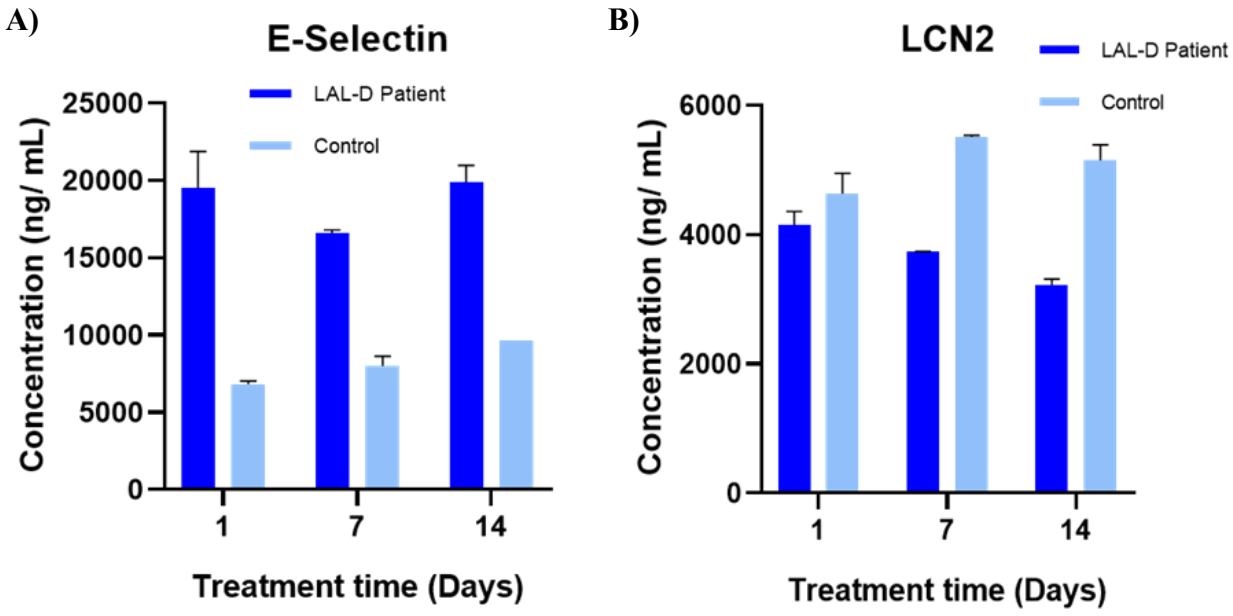

*Figure 23. E-Selectin (**A**) and LCN2 (**B**) concentration (ng/mL) of LAL-D patient and of healthy individual at three different times, by duplicate. LCN2: Lipocalin-2; LAL-D: Lysosomal Acid Lipase Deficiency.*

LRP1 and IL-1B macrophages protein expression

The next step, following the same line, was time for Western Blot: This analysis was conducted to evaluate the expression levels of LRP1 and IL-1β in macrophages derived from both a healthy individual and a patient with LAL-D, in order to identify potential changes resulting from drug administration. Protein abundance was quantified by densitometry, and values were normalized to actin to account for loading variability, as

recommended for accurate and reproducible quantification. For both LRP1 and IL1-β, the normalized expression (protein/actin ratio) was calculated for each condition. The results are presented as fold change relative to the respective control condition within each group.

Representative immunoblots and corresponding densitometric quantification graphs are shown in Figures 24, 25, 26, 27, 28, 29. These results reveal differential regulation of LRP1 and IL1-β between healthy individual and LAL-D macrophages, highlighting disease-specific alterations in protein expression. The tables used to create the graphs are attached in Annex III.

Regarding LRP1, the Figures 24, 25 and 26 shows the evolution of the protein expression of LAL-D patient and of Healthy individual in macrophages, relative to control, across different lipoprotein incubation conditions (untreated control, LDL, and VLDL) at days 1, 7, and 14.

For the LAL-D patient (Figure 25, Panel A) the graph shows that LRP1 protein expression. At day 1, the fold change is slightly above 1 for both VLDL incubation, with a more pronounced increase in the LDL condition, indicating higher LRP1 expression in LAL-D macrophages compared to healthy controls immediately after LDL exposure. At day 7, both VLDL and LDL conditions remain similar to day 1. By day 14, the fold increases for VLDL and LDL remain elevated compared to control, reaching the highest values observed indicating an upregulation of LRP1 in LAL-D macrophages.

For the healthy individual (Figure 25, Panel B) at day 1, both VLDL and LDL treatments result in a fold increase near 1, indicating similar LRP1 expression levels between treated and untreated healthy macrophages. At day 7, there is an increase in the fold increase for both VLDL and LDL, but these values remain higher than those observed in the LAL-D group. By day 14, the fold increases for both lipoprotein treatments remain below LAL-D patient levels.

In order to compare the degree of LRP1 expression between the LAL-D patient and the healthy individual, we proceed to extrapolate it in a graph presented as fold increase relative to the control condition at each time point (Figure 26). Overall, we observed an increased expression of the LRP1 protein in the LAL-D patient on days 1 and 14 compared to our healthy control, whereas on day 7, a higher expression was noted in the healthy control.

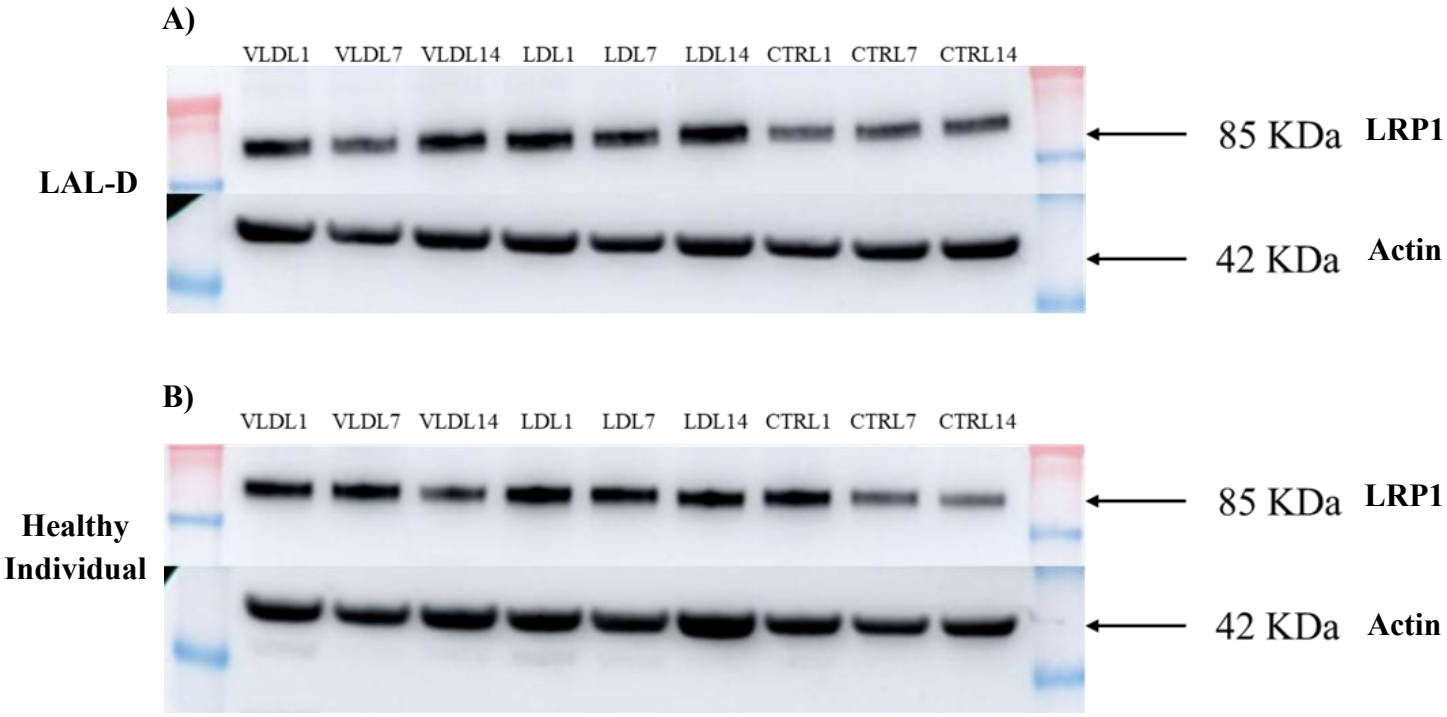

*Figure 24. Representative Western blot analysis of LRP1 expression in macrophages derived from a LAL-D patient (**A**) and from a healthy individual (**B**). The upper panel shows immunodetection of LRP1 (85 kDa), and the lower panel shows actin (42 kDa) as a loading control. Samples correspond to macrophages incubated with VLDL (150 µg/mL) (lanes 1–3: days 1, 7, and 14), LDL (150 µg/mL) (lanes 4–6: days 1, 7, and 14), and untreated control (lanes 7–9: days 1, 7, and 14). Molecular weight markers are indicated on the right. LAL-D: Lysosomal Acid Lipase Deficiencyl; LDL: Low-density lipoprotein; VLDL: Very low-density lipoprotein; CTRL: Control (no-lipoprotein)*

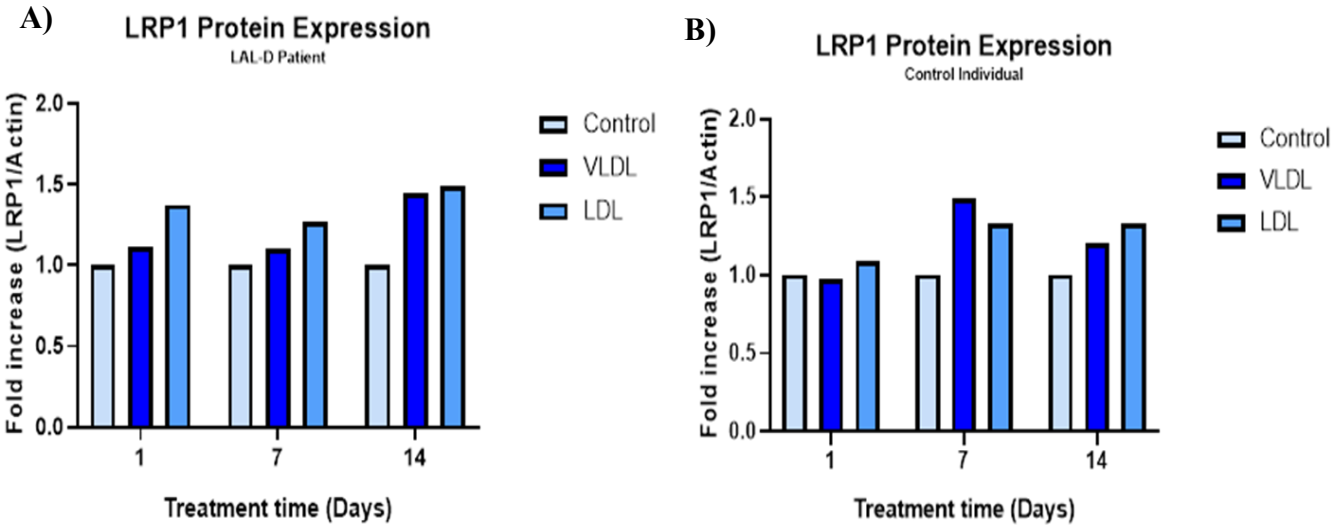

*Figure 25. Quantification of LRP1 protein expression normalized to actin in macrophages from a LAL-D patient (**A**) and a healthy individual (**B**) under different lipoprotein treatments (VLDL (150 µg/mL), LDL (100 µg/mL), and untreated control) at days 1, 7, and 14. Data are presented as fold change relative to the control condition (=1) at each time point. LAL-D: Lysosomal Acid Lipase Deficiency; LDL: Low-density lipoprotein; VLDL: Very low-density lipoprotein*

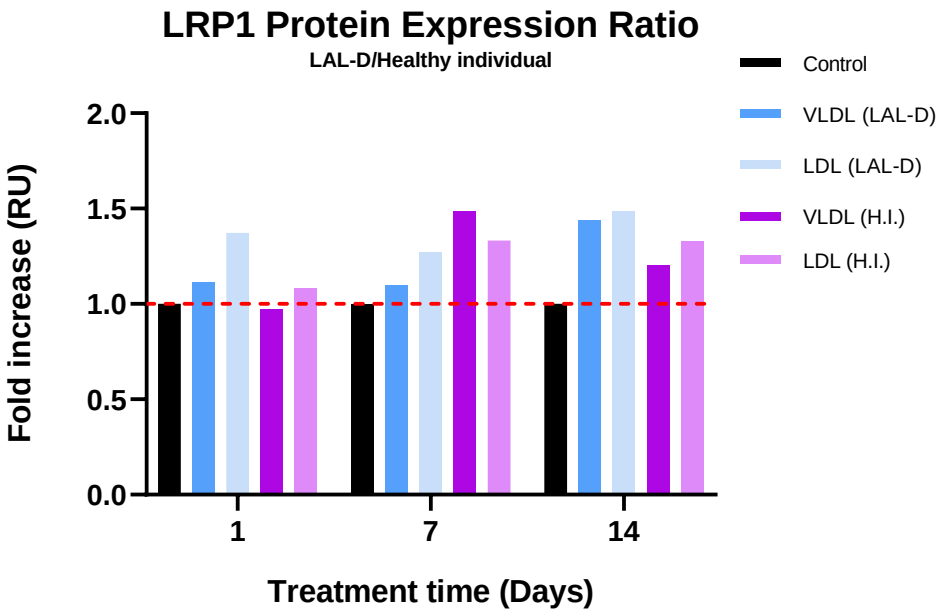

Figure 26. Quantification of LRP1 protein of LAL-D patient and healthy individual in macrophages over time. The bar graph shows the fold increase in LRP1 protein expression relative to control under different lipoprotein incubation conditions (VLDL (150 µg/mL) and LDL (100 µg/mL)) at days 1, 7, and 14. The black bar represents the no-incubated control. Light and dark blue bars indicate VLDL and LDL incubation in LAL-D macrophages, respectively, while light and dark purple bars represent VLDL and LDL incubation in healthy individual (H.I.) macrophages. The red dashed line marks a ratio of 1 (no change relative to control). LAL-D: Lysosomal Acid Lipase Deficiency; H.I.: Healthy Individual; LDL: Low-density lipoprotein; VLDL: Very low-density lipoprotein

Regarding IL-1β expression the Figures 27, 28 and 29 shows the evolution of the protein expression of LAL-D patient and of Healthy individual in macrophages, relative to control, across different lipoprotein incubation conditions (untreated control, LDL, and VLDL) at days 1, 7, and 14.

In LAL-D macrophages (Figure 28 panel A), IL-1β expression remains close to the baseline across mostly conditions and time points. At day 1, both VLDL and LDL treatments result in only minor changes in IL-1β levels compared to the control. At day 7 IL-1β expression remains under baseline and at day 14, there is a slight increase in IL-1β expression after VLDL and incubation, but the fold changes are consistently lower than those observed in the healthy individual group. This indicates that, unlike healthy macrophages, LAL-D macrophages display a blunted IL-1β response to lipoprotein stimulation over time.

In macrophages from the healthy individual (Figure 28 panel B), IL-1β protein expression shows a marked increase after incubation with VLDL and LDL, especially at days 7 and 14. At day 1, there is already a moderate elevation in IL-1β expression following VLDL incubation. This increase becomes more pronounced on day 7, where both VLDL and LDL conditions reach the highest fold increase is observed in the entire dataset, indicating a strong inflammatory response. By day 14, IL-1β expression remains elevated in the healthy individual after both VLDL and LDL treatments, although the values are slightly lower than at day 7.

In order to compare the degree of IL-1 β expression between the LAL-D patient and the healthy individual, we proceed to extrapolate it in a graph presented as fold increase relative to the control condition at each time point (Figure 29). Overall, we observed an decreased expression of the IL-1β protein in the LAL-D patient during the 15-days treatment compared to our healthy control.

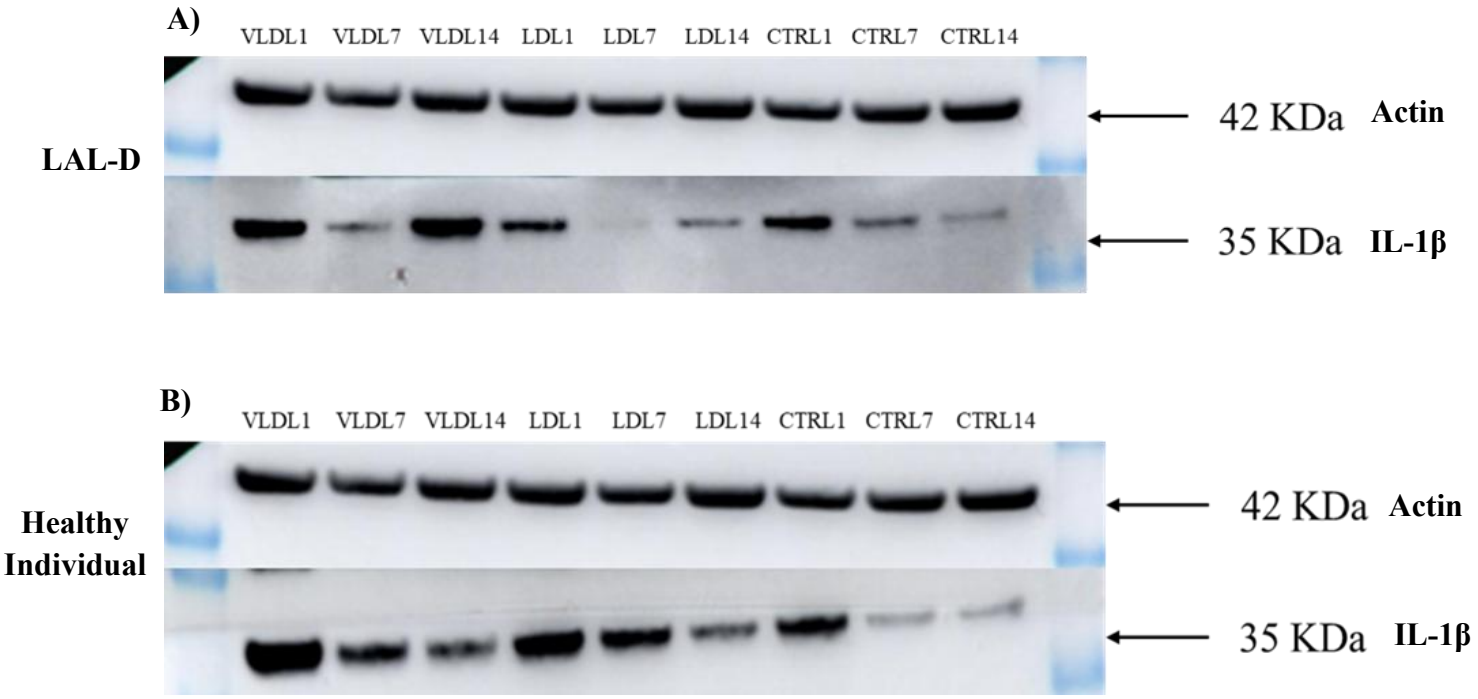

*Figure 27 Representative Western blot analysis of IL-1β expression in macrophages derived from a LAL-D patient (**A**) and from a healthy individua (**B**)l. The upper panel shows immunodetection of actin (42 kDa), as a loading control, and the lower panel shows IL-1β (35 kDa). Samples correspond to macrophages incubated with VLDL (150 µg/mL) (lanes 1–3: days 1, 7, and 14), LDL (100 µg/mL) (lanes 4–6: days 1, 7, and 14), and untreated control (lanes 7–9: days 1, 7, and 14). Molecular weight markers are indicated on the right. LAL-D: Lysosomal Acid Lipase Deficiency; CTRL: Control (no-lipoprotein); LDL: Low-density lipoprotein; VLDL: Very low-density lipoprotein.*

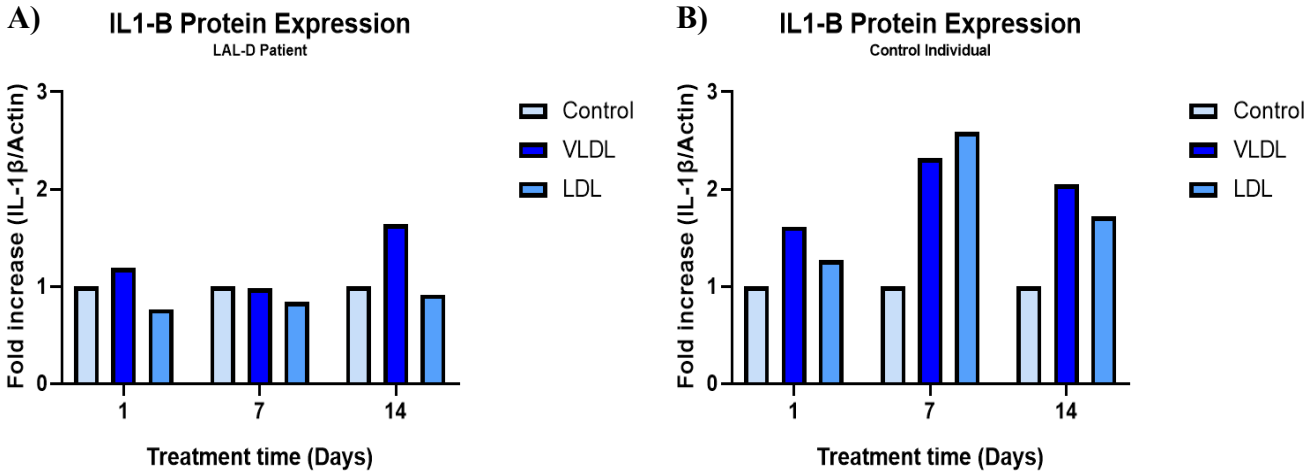

*Figure 28. Quantification of IL-1β protein expression normalized to actin in macrophages from a LAL-D patient (**A**) and from a healthy individual (**B**) under different lipoprotein treatments (VLDL (150 µg/mL), LDL (100 µg/mL), and untreated control) at days 1, 7, and 14. Data are presented as fold change relative to the control condition (=1) at each time point. LAL-D: Lysosomal Acid Lipase Deficiency; LDL: Low-density lipoprotein; VLDL: Very low-density lipoprotein*

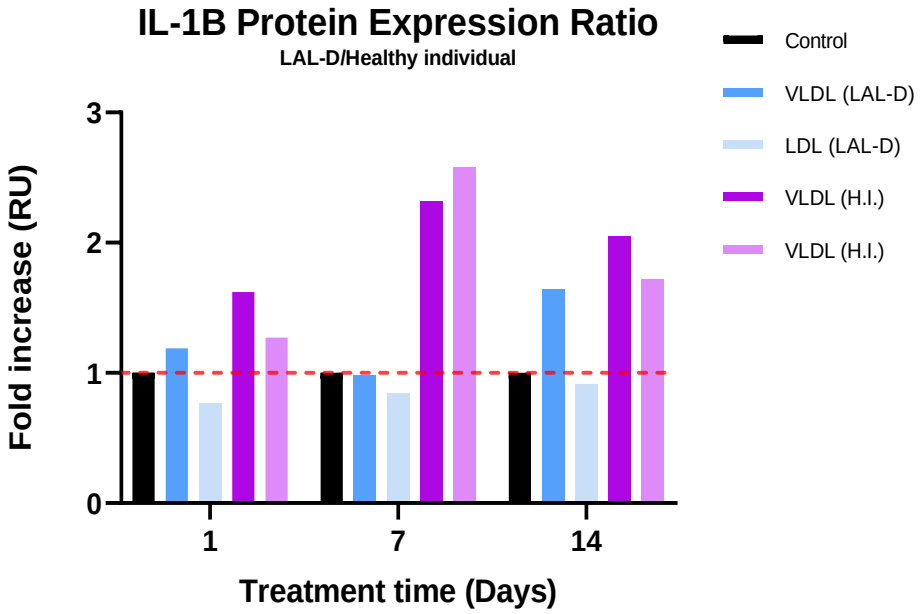

Figure 29. Quantification of IL-1β protein expression ratio (LAL-D/Healthy individual) in macrophages over time. The bar graph shows the fold increase in IL-1β protein expression (LAL-D patient relative to healthy individual) under different lipoprotein incubation conditions (VLDL (150 µg/mL) and LDL (100 µg/mL)) at days 1, 7, and 14. The black bar represents the no-incubated control. Light and dark blue bars indicate VLDL and LDL incubation in LAL-D macrophages, respectively, while light and dark purple bars represent VLDL and LDL incubation in healthy individual (H.I.) macrophages. The red dashed line marks a ratio of 1 (no change relative to control). LAL-D: Lysosomal Acid Lipase Deficiency; H.I.: Healthy Individual; LDL: Low-density lipoprotein; VLDL: Very low-density lipoprotein

7. DISCUSSION

Currently, the relationship between LAL-D and atherosclerosis is well established and is primarily attributed to the dyslipidemia caused by the disease. Specifically, this is due to the increase in pro-atherogenic molecules such as LDL-C and TG, as well as the decrease in HDL-C, one of the main anti-atherogenic lipoproteins. For this reason, the aim is to determine whether treatment with Sebelipase α can improve the harmful profile associated with atherosclerosis. However, the objective is not limited to addressing dyslipidemia alone; we also seek to support this hypothesis by investigating additional related factors and mechanisms.

Regarding the first objective, the findings presented in lipidic determination illustrate a normalization of most parameters as the days under treatment progressed. Considering that the values associated with the progression of atherosclerosis (LDL-C, the main causes of atheromatous plaque, or TG) are enhanced in the LAL-D patient than in healthy control, that results suggest a lower exposure to those lipoproteins or particles involved in the progression of atherosclerosis as the treatment progresses.

With these results we contrast those already reported, that treatment with Sebelipase α reduces LDL-C, LDL particle number and TG suggesting an improvement of atherogenic profile (Siuffi-Campo et al. 2022), especially due to the reduction of de novo cholesterol synthesis. Considering the percentages of decrease, it is clearly seen how the values of the LAL-D patient are more variable with respect to our control.

Following the results of transaminases that indicate possible liver damage (typical of LAL-D patients), we can observe that GGT, an enzyme found mainly in the liver and commonly used as a biomarker for liver function and could be related with atherosclerosis via inflammatory mechanisms (Li et al. 2024), is persistently decreased during 15-day ERT. This decrease could be explained by the functionality of the ERT with Sebelipase α, so that by replacing the defective enzyme, the breakdown of accumulated lipids is favored, thus rapidly reducing hepatic inflammation. On other hand, the decrease in GPT could be explained by its association with hepatocyte cell damage (Li et al. 2024), explaining its decrease too. In any case, the results should be contrasted with a larger number of patients to obtain robust conclusions. Following with uCPR results, although it decreases as the days of treatment pass, it can be observed that it always remains above control levels. The higher concentration may be due to the fact that it is an acute-phase protein produced by the liver in response to inflammation (it serves as a biomarker for systemic inflammation and is used to assess inflammatory activity) (Soeki and Sata 2016) and may be higher at the beginning due to the action of the ERT and the high activity of LAL in breaking down lipid esters. Similarly, the assay would need to be reproduced in a longer time to demonstrate the relationship between Sebelipase α with atherosclerosis.

Regarding the Liposcale+ Test, represented in Figure 15, it provides a comparison of the lipid profile between the LAL-D patient during 15-day ERT, at three different times, and a healthy control. In the LAL-D patient, the profiles consistently show a distinct pattern

compared to the healthy control. Notably, the LAL-D patient shows higher values for parameters associated with atherogenic risk, such as LDL-C, LDL-TG, and remanent cholesterol, as indicated by the continue orange lines across all time points. These findings are consistent with the pathophysiology of LAL-D, where impaired LAL activity leads to the accumulation of CE and TG within tissues and plasma, despite receiving ERT (Burton et al. 2015). The control individual, exhibits a more stable profile in time, with most parameters remaining within the reference range (green dots), referencing the efficient lipid metabolism and a lower cardiovascular risk. The differences are evident in the LDL parameters and cholesterol, which are markedly elevated in the LAL-D patient. Switching to HDL-related parameters (HDL-C, medium-HDL-P, HDL-Ø) appear relatively stables in both groups. The glycoprotein markers Glyc-A and Glyc-B (low-degree systemic inflammation biomarkers) also remain within normal limits, suggesting that the primary metabolic disfunction in LAL-D is centered on the atherogenic lipoproteins. In summary, as we can observe on day 14 of treatment, the Liposcale representation deviates less from the reference line, suggesting an improvement of the atherosclerotic profile, decreasing the risk.

Regarding the comparison between the 89-population and the LAL-D patient, we can confirm, similarly to what was observed with the healthy control, that the levels of pro-atherogenic molecules are elevated. Likewise, we can also observe that, as the days of ERT progress in the LAL-D patient, the levels of these molecules tend to decrease, suggesting a reduced cardiovascular risk and a slower progression of atherosclerosis. We could then determine that the treatment, comparing the values with those of the control and the reference population, improves the lipoprotein profile as well as the cardiovascular risk.

Following with plasmatic biomarkers, and regarding E-Selectin results, it shows that E-selectin concentration is consistently higher in the LAL-D patient during the 15 days of ERT treatment compared to the healthy control. E-selectin is an endothelial adhesion molecule induced by proinflammatory cytokines, and its elevation reflects endothelial activation and a vascular inflammatory state, both processes involved in the progression of atherosclerosis (Galkina and Ley 2007), so persistently high levels in the LAL-D patient suggest that, despite ERT treatment, significant endothelial activation persists, which could indicate an elevated residual vascular risk in these patients that may account for additional cardiovascular risk besides an relative normal lipoprotein profile.

The pharmacodynamic response to ERT could explain the E-Selectin concentration from LAL-D patient samples. Between days 1 and 14, E-selectin concentrations appear to remain relatively similar, with the lowest peak observed on day 7, while consistently remaining above healthy control levels. This decrease could be related to a high functional activity of recombinant LAL, reflecting a general reduction in inflammation, which returns to baseline the day before the next administration of Sebelipase α. After endothelial cell stimulation, newly synthesized E-selectin is rapidly detected (Mantovani and Dejana 1998). Its expression begins approximately 3-4 hours after inflammatory

stimulation and returns to basal levels within 16-24 hours. This rapid kinetic allows E-selectin levels to reflect acute changes in endothelial activation, such as those that may occur after Sebelipase α administration.

In contrast, levels of LCN2, an acute-phase protein associated with inflammation and recognized as a sensitive biomarker of both acute and chronic liver injury, were consistently lower in LAL-D patients compared to healthy controls throughout the study period. LCN2 levels from LAL-D patient remains under healthy control levels at three different times and follows a downward trend as the number of days increases. Since LCN2 is typically elevated during hepatic stress, inflammation, or functional failure (Asimakopoulou, Weiskirchen, and Weiskirchen 2016) and this reduction could suggest that ERT exerts a beneficial effect by attenuating acute hepatic injury and suppressing LCN2 expression, or that the underlying disease limits an adequate hepatic inflammatory response.

Taken together, these observations indicate that while ERT does not fully reverse endothelial activation in LAL-D (as demonstrated by persistently elevated E-selectin), it may attenuate acute hepatic stress, as suggested by reduced LCN2 levels. Overall, the results reveal a complex inflammatory and immunometabolic profile in LAL-D patients under ERT, distinct from that observed in healthy individuals. Based on previously conducted and published studies, it is well established that treatment with Sebelipase α can improve both the lipidic and hepatic profiles (Balwani et al. 2013). Therefore, our objective of demonstrating that the treatment also improves the atherosclerotic profile is strongly limited by the number of patients in the study of this ultra-rare disorder and the duration over which it is conducted. In order to obtain more accurate conclusions, reproduction of the trial in a larger number of patients and over a longer period of time is necessary

In reference to our second objective, macrophages were differentiated from PBMCs and incubated with lipoproteins in order to determine differences between the behavior of those of the LAL-D patient and the control individual during the 15-days course of the treatment. Differentiated macrophages from both LAL-D patient and healthy individual were incubated with both VLDL+IDL and LDL and this internalization was compared at three different times from the ERT, using Nile Red staining to visualize it.

LAL-D is characterized by a deficiency in LAL, which is essential for hydrolyzing CE and TG. Treatment with Sebelipase α leads to a breakdown of internalized lipids (CE and TG). The enhanced hydrolysis, resulting in elevated FC concentration, may lead to feedback mechanisms that downregulate LDL receptor expression (Errico et al. 2013), (which is normal in healthy patients but is increased in LAL-D patients in ERT) further reducing intracellular lipid droplet formation. As a result, macrophages from LAL-D patients show limited accumulation of neutral lipid droplets, as evidenced by Nile Red fluorescence, because the internalized lipids are efficiently processed and stored.

In contrast, macrophages from healthy control show robust Nile Red fluorescence under all conditions, reflecting their intact capacity for lipid uptake, hydrolysis, and storage.

Upon incubation with LDL or VLDL, these cells efficiently internalize lipoprotein-derived lipids, process them in functional lysosomes, and accumulate numerous, brightly fluorescent lipid droplets. This dynamic response is especially evident after VLDL exposure and at later time points, highlighting the healthy macrophages' ability to adapt to increased lipid availability and maintain effective lipid homeostasis.

Another reason that could explain the poor lipid internalization, especially LDL, could be that macrophages express receptors for VLDL and, above all, for modified LDL (mainly oxidized LDL), known as scavenger receptors. These receptors are not regulated by the intracellular cholesterol content and allow excessive lipid accumulation, which contributes to the formation of foam cells (de Gonzalo-Calvo, Revuelta-López, and Llorente-Cortés 2013). The classical LDL receptor, which recognizes native LDL, is poorly expressed in mature macrophages. Therefore, the uptake of native LDL by macrophages is limited, whereas the uptake of oxidized LDL is much higher thanks to scavenger receptors. In contrast, VLDL uptake may be more efficient in macrophages because there are VLDL-specific receptors (such as LRP1) that recognize apoE-rich particles and are not down-regulated by intracellular cholesterol and do not need previous modifications of the VLDL particle for its internalization.

An important point to note is that in healthy individuals, efficient internalization of LDL and VLDL by macrophages and subsequent foam cell formation is a key step in atherosclerotic plaque formation and progression. As we can observe, the internalization of VLDL and LDL in the LAL-D patient, apart from being lower, is trending downward. This tendency could suggest that the effect obtained thanks to the action of Sebelipase α would be the improvement of the atherosclerotic profile.

In order to demonstrate our hypothesis by carrying out the third objective and following with the results obtained by Western Blot from cellular extracts, the quantified protein expressions were LRP1 and IL-1β.

Regarding LRP1 expression, that is a multifunctional receptor that mediates the uptake of a wide range of ligands, mainly apoE-rich lipoproteins such as found in VLDL and plays a key role in the internalization of esterified cholesterol derived from VLDL (Escolà Gil 2012). Starting with LRP1 concentration of macrophages from LAL-D patient, its expression is consistently at or above the healthy control level for all conditions and time points, with the most marked increase after LDL exposure, and this upregulation persists or intensifies over time.

In contrast, healthy macrophages show little change in LRP1 expression after lipoprotein treatment at day 1, a moderate increase by day 7, and by day 14, their LRP1 levels under LDL/VLDL remain below those of LAL-D macrophages. Notably, after LDL incubation, LRP1 expression in LAL-D macrophages is already elevated at day 1 and remains high or increases further at days 7 and 14.

In this case, LRP1 expression is found to be slightly increased in the LAL-D patient, this could be explained as a potential mechanism to counteract the stress caused by the high

concentration of lipoproteins with which the macrophages are incubated even though what we observe through Nile Red fluorescence indicates a much lower level of internalization. On the other hand, LAL-D patients tend to overexpress lipoprotein receptors in response to intracellular lipid accumulation. Therefore, the increased expression of the LRP1 protein observed as the days of treatment progress can be associated with the pharmacodynamics of the therapy, with the peak expression occurring precisely the day before the next administration (Figure 25, panel A). However, results cannot be extrapolated based on a single replicate and a single patient, so repeating the experiment with a larger number of patients and a longer duration of ERT is necessary.

Regarding IL-1β expression, it is a key pro-inflammatory cytokine involved in the pathogenesis of atherosclerosis. It is primarily produced by macrophages, vascular smooth muscle cells, and other immune cells in response to stimuli such as the presence of atherogenic lipids (Viana-Huete and Fuster 2019). Starting with macrophages derived from the LAL-D patient, the IL-1β protein expression fold change remains close to or slightly above 1 (referencing control as 1) cross all time points and lipoprotein treatments. At day 1, both VLDL and LDL incubations result in fold increases near or just above the baseline, indicating that IL-1β expression in LAL-D macrophages is similar to, or only marginally higher than in healthy controls. This pattern persists at day 7, with ratios for both VLDL and LDL still hovering around 1, suggesting that exposure to these lipoproteins does not strongly upregulate IL-1β. By day 14, there is a modest increase in the ratio for VLDL, but the values remain well below those observed in healthy macrophages exposed to the same lipoproteins. This muted inflammatory response may reflect the effects of ERT and ezetimibe in reducing lysosomal lipid accumulation and dampening pro-inflammatory signaling pathways in LAL-D macrophages.

In contrast, macrophages from the healthy individual display a much more pronounced increase in IL-1β protein expression depending on lipoprotein exposure and indicating a sustained inflammatory response in healthy macrophages when exposed to high levels of VLDL or LDL. This suggests that healthy macrophages are more reactive to lipid-induced stress, rapidly activating pro-inflammatory pathways such as those leading to IL-1β production. In summary, the reduced expression of proteins typically elevated during pro atherosclerotic processes may indicate a potential anti-atherogenic effect in the LAL-D patient under Sebelipase α treatment.

It is important to highlight that the results obtained represents only the beginning of a wide range of research possibilities, and that this assay should be replicated with a larger patient cohort and over a longer period of time in order to draw solid conclusions.

8. CONCLUSION

The three objectives of this study were designed to provide an evaluation of the impact of Sebelipase α ERT on the atherosclerotic profile of a LAL-D patient. The results obtained align closely with these aims and support the initial hypothesis.

Regarding the objective 1, was focused on the analysis of the lipid and hepatic profiles in a LAL-D patient compared to a healthy control, across three time points following Sebelipase α administration. The findings show progressive normalization of lipid levels (LDL-C, TG) and improved liver function (lower GGT), indicating ERT's positive impact on cholesterol synthesis and metabolism.

About objective 2, was addressed the isolation and differentiation of macrophages to evaluate their behavior and capacity for lipid internalization and its relation to atherogenesis. ERT with Sebelipase α reduced lipid uptake in LAL-D macrophages and lowered IL-1β expression, suggesting it may limit foam cell formation and inflammation: key processes in atherosclerosis.

Finally, objective 3 aimed to assess atherosclerosis-related biomarkers in both plasma and macrophages. The conclusions highlight that biomarkers like E-selectin, LRP1, and LCN2 reflect treatment-related changes, with overall improvement in inflammation and atherogenic risk despite persistent endothelial activation.

In summary, Sebelipase α shows multidimensional benefits in LAL-D, impacting both lipid levels and atherosclerosis-related biomarkers. Larger studies are needed to confirm these findings and guide atherosclerotic risk management.

9. BIBLIOGRAPHY

Aguisanda, Francis, Natasha Thorne, and Wei Zheng. 2017. "Targeting Wolman Disease and Cholesteryl Ester Storage Disease: Disease Pathogenesis and Therapeutic Development." *Current chemical genomics and translational medicine* 11: 1–18. doi:10.2174/2213988501711010001.

Anderson, Richard A., Nagesh Rao, Robert S. Byrum, Cynthia B. Rothschild, Donald W. Bowden, Rosa Hayworth, and Mark Pettenati. 1993. "In Situ Localization of the Genetic Locus Encoding the Lysosomal Acid Lipase/Cholesteryl Esterase (LIPA) Deficient in Wolman Disease to Chromosome 10q23.2-Q23.3." *Genomics* 15(1): 245–47. doi:10.1006/geno.1993.1052.

Asimakopoulou, Anastasia, Sabine Weiskirchen, and Ralf Weiskirchen. 2016. "Lipocalin 2 (LCN2) Expression in Hepatic Malfunction and Therapy." *Frontiers in Physiology* 7. doi:10.3389/fphys.2016.00430.

Balwani, Manisha, Catherine Breen, Gregory M. Enns, Patrick B. Deegan, Tomas Honzík, Simon Jones, John P. Kane, et al. 2013. "Clinical Effect And Safety Profile of Recombinant Human Lysosomal Acid Lipase in Patients With Cholesteryl Ester Storage Disease." *Hepatology* 58(3): 950–57. doi:10.1002/hep.26289.

Benitez Amaro, Aleyda, Angels Solanelles Curco, Eduardo Garcia, Josep Julve, Jose Rives, Sonia Benitez, and Vicenta Llorente Cortes. 2021. "Apolipoprotein and LRP1-Based Peptides as New Therapeutic Tools in Atherosclerosis." *Journal of clinical medicine* 10(16). doi:10.3390/jcm10163571.

Bernstein, Donna L, Helena Hülkova, Martin G Bialer, and Robert J Desnick. 2013. "Cholesteryl Ester Storage Disease: Review of the Findings in 135 Reported Patients with an Underdiagnosed Disease." *Journal of hepatology* 58(6): 1230–43. doi:10.1016/j.jhep.2013.02.014.

Besler, Katrina J., Valentin Blanchard, and Gordon A. Francis. 2022. "Lysosomal Acid Lipase Deficiency: A Rare Inherited Dyslipidemia but Potential Ubiquitous Factor in the Development of Atherosclerosis and Fatty Liver Disease." *Frontiers in Genetics* 13. doi:10.3389/fgene.2022.1013266.

Burton, Barbara K, Patrick B Deegan, Gregory M Enns, Ornella Guardamagna, Simon Horslen, Gerard K Hovingh, Steve J Lobritto, et al. 2015. "Clinical Features of Lysosomal Acid Lipase Deficiency." *Journal of pediatric gastroenterology and nutrition* 61(6): 619–25. doi:10.1097/MPG.0000000000000935.

Camarena, Carmen, Luis J. Aldamiz-Echevarria, Begoña Polo, Miguel A. Barba Romero, Inmaculada García, Jorge J. Cebolla, and Emilio Ros. 2017. "Update on Lysosomal Acid Lipase Deficiency: Diagnosis, Treatment and Patient Management." *Medicina Clínica (English Edition)* 148(9): 429.e1-429.e10. doi:10.1016/j.medcle.2017.04.021.

Chen, Jiegen, Josepmaria Argemi, Gemma Odena, Ming-Jiang Xu, Yan Cai, Veronica Massey, Austin Parrish, et al. 2020. “Hepatic Lipocalin 2 Promotes Liver Fibrosis and Portal Hypertension.” *Scientific Reports* 10(1): 15558. doi:10.1038/s41598-020-72172-7.

Chuang, Jen-Chieh, Adam M. Lopez, Kenneth S. Posey, and Stephen D. Turley. 2014. “Ezetimibe Markedly Attenuates Hepatic Cholesterol Accumulation and Improves Liver Function in the Lysosomal Acid Lipase-Deficient Mouse, a Model for Cholesteryl Ester Storage Disease.” *Biochemical and Biophysical Research Communications* 443(3): 1073–77. doi:10.1016/j.bbrc.2013.12.096.

Dubland, Joshua A, and Gordon A Francis. 2015. “Lysosomal Acid Lipase: At the Crossroads of Normal and Atherogenic Cholesterol Metabolism.” *Frontiers in cell and developmental biology* 3: 3. doi:10.3389/fcell.2015.00003.

Errico, Teresa L., Xiangyu Chen, Jesús M. Martin Campos, Josep Julve, Joan Carles Escolà-Gil, and Francisco Blanco-Vaca. 2013. “Mecanismos Básicos: Estructura, Función y Metabolismo de Las Lipoproteínas Plasm.” *Clínica e Investigación en Arteriosclerosis* 25(2): 98–103. doi:10.1016/j.arteri.2013.05.003.

Erwin, Angelika L. 2017. “The Role of Sebelipase Alfa in the Treatment of Lysosomal Acid Lipase Deficiency.” *Therapeutic advances in gastroenterology* 10(7): 553–62. doi:10.1177/1756283X17705775.

Escolà Gil, Joan Carles. 2012. “El Receptor LRP1 Media La Captación y Acumulación Del Colesterol Esterificado de Las VLDL Inducido Por La Hipoxia En Cardiomiocitos.” *Clínica e Investigación en Arteriosclerosis* 24(6): 306–7. doi:10.1016/j.arteri.2012.09.007.

European Medicines Agency. 2024. “Product Information: Kanuma® (Sebelipase Alfa).” *https://www.ema.europa.eu/en/documents/product-information/kanuma-epar-product-information_en.pdf*.

Galkina, Elena, and Klaus Ley. 2007. “Vascular Adhesion Molecules in Atherosclerosis.” *Arteriosclerosis, Thrombosis, and Vascular Biology* 27(11): 2292–2301. doi:10.1161/ATVBAHA.107.149179.

de Gonzalo-Calvo, David, Elena Revuelta-López, and Vicenta Llorente-Cortés. 2013. “Mecanismos Básicos. Regulación y Aclaramiento de Las Lipoproteínas Que Contienen ApolipoproteínaB.” *Clínica e Investigación en Arteriosclerosis* 25(4): 194–200. doi:10.1016/j.arteri.2013.05.002.

Guerreiro, Gilian, Marion Deon, and Carmen Regla Vargas. 2023. “Evaluation of Biochemical Profile and Oxidative Damage to Lipids and Proteins in Patients with Lysosomal Acid Lipase Deficiency.” *Biochemistry and Cell Biology* 101(4): 294–302. doi:10.1139/bcb-2022-0330.

Hamilton, John, Iain Jones, Rajeev Srivastava, and Peter Galloway. 2012. “A New Method for the Measurement of Lysosomal Acid Lipase in Dried Blood Spots Using the Inhibitor Lalistat 2.” *Clinica Chimica Acta* 413(15–16): 1207–10. doi:10.1016/j.cca.2012.03.019.

Heltianu, Constantina, Alexandra Robciuc, Gabriela Botez, Claudia Musina, Camelia Stancu, Anca V Sima, and Maya Simionescu. 2011. “Modified Low Density Lipoproteins Decrease the Activity and Expression of Lysosomal Acid Lipase in Human Endothelial and Smooth Muscle Cells.” *Cell biochemistry and biophysics* 61(1): 209–16. doi:10.1007/s12013-011-9190-8.

Jones, Simon A., Sandra Rojas-Caro, Anthony G. Quinn, Mark Friedman, Sachin Marulkar, Fatih Ezgu, Osama Zaki, et al. 2017. “Survival in Infants Treated with Sebelipase Alfa for Lysosomal Acid Lipase Deficiency: An Open-Label, Multicenter, Dose-Escalation Study.” *Orphanet Journal of Rare Diseases* 12(1): 25. doi:10.1186/s13023-017-0587-3.

Korbelius, Melanie, Katharina B Kuentzel, Ivan Bradić, Nemanja Vujić, and Dagmar Kratky. 2023. “Recent Insights into Lysosomal Acid Lipase Deficiency.” *Trends in molecular medicine* 29(6): 425–38. doi:10.1016/j.molmed.2023.03.001.

Lam, Patricia, Deborah A Zygmunt, Anna Ashbrook, Cong Yan, Hong Du, and Paul T Martin. 2024. “Liver-Directed AAV Gene Therapy Normalizes Disease Symptoms and Provides Cross-Correction in a Model of Lysosomal Acid Lipase Deficiency.” *Molecular therapy : the journal of the American Society of Gene Therapy* 32(12): 4272–84. doi:10.1016/j.ymthe.2024.10.022.

de las Heras, Javier, Carolina Almohalla, Javier Blasco-Alonso, Mafalda Bourbon, Maria-Luz Couce, María José de Castro López, Mª Concepción García Jiménez, et al. 2024. “Practical Recommendations for the Diagnosis and Management of Lysosomal Acid Lipase Deficiency with a Focus on Wolman Disease.” *Nutrients* 16(24): 4309. doi:10.3390/nu16244309.

Li, Chun, Long Gu, Fu-Yi Shi, Shi-Ying Xiong, Gui-Sheng Wu, Jian-Hua Peng, Ruo-Lan Wang, et al. 2024. “Serum Liver Enzymes and Risk of Stroke: Systematic Review with Meta-Analyses and Mendelian Randomization Studies.” *European journal of neurology* 31(12): e16506. doi:10.1111/ene.16506.

Malinová, Věra, Manisha Balwani, Reena Sharma, Jean-Baptiste Arnoux, John Kane, Chester B. Whitley, Sachin Marulkar, and Florian Abel. 2020. “Sebelipase Alfa for Lysosomal Acid Lipase Deficiency: 5-year Treatment Experience from a Phase 2 Open-label Extension Study.” *Liver International* 40(9): 2203–14. doi:10.1111/liv.14603.

Mantovani, Alberto, and Elisabetta Dejana. 1998. “Endothelium.” In *Encyclopedia of Immunology*, Elsevier, 802–6. doi:10.1006/rwei.1999.0212.

Pajares, Sonia, Angela Arias, Judit García-Villoria, Judit Macías-Vidal, Emilio Ros, Javier de las Heras, Marisa Girós, Maria J. Coll, and Antonia Ribes. 2015. "Cholestane-3β,5α,6β-Triol: High Levels in Niemann-Pick Type C, Cerebrotendinous Xanthomatosis, and Lysosomal Acid Lipase Deficiency." *Journal of Lipid Research* 56(10): 1926–35. doi:10.1194/jlr.M060343.

Pisciotta, Livia, Raffaele Fresa, Antonella Bellocchio, Elisabetta Pino, Virgilia Guido, Alfredo Cantafora, Maja Di Rocco, Sebastiano Calandra, and Stefano Bertolini. 2009. "Cholesteryl Ester Storage Disease (CESD) Due to Novel Mutations in the LIPA Gene." *Molecular Genetics and Metabolism* 97(2): 143–48. doi:10.1016/j.ymgme.2009.02.007.

Prasad, Kailash, and Manish Mishra. 2022. "Mechanism of Hypercholesterolemia-Induced Atherosclerosis." *Reviews in cardiovascular medicine* 23(6): 212. doi:10.31083/j.rcm2306212.

Reiner, Željko, Ornella Guardamagna, Devaki Nair, Handrean Soran, Kees Hovingh, Stefano Bertolini, Simon Jones, et al. 2014. "Lysosomal Acid Lipase Deficiency--an under-Recognized Cause of Dyslipidaemia and Liver Dysfunction." *Atherosclerosis* 235(1): 21–30. doi:10.1016/j.atherosclerosis.2014.04.003.

Ridker, Paul M, Brendan M. Everett, Tom Thuren, Jean G. MacFadyen, William H. Chang, Christie Ballantyne, Francisco Fonseca, et al. 2017. "Antiinflammatory Therapy with Canakinumab for Atherosclerotic Disease." *New England Journal of Medicine* 377(12): 1119–31. doi:10.1056/NEJMoa1707914.

Ruiz-Andrés, Carla, Elena Sellés, Angela Arias, and Laura Gort. 2017. "Lysosomal Acid Lipase Deficiency in 23 Spanish Patients: High Frequency of the Novel c.966+2T>G Mutation in Wolman Disease." In , 7–12. doi:10.1007/8904_2017_6.

Saito, Seiji, Kazuki Ohno, Toshihiro Suzuki, and Hitoshi Sakuraba. 2012. "Structural Bases of Wolman Disease and Cholesteryl Ester Storage Disease." *Molecular genetics and metabolism* 105(2): 244–48. doi:10.1016/j.ymgme.2011.11.004.

Scott, SA. 2013. "Frequency of the Cholesteryl Ester Storage Disease Common LIPA E8SJM Mutation (c. 894G> A) in Various Racial and Ethnic Groups." *Hepatology* 58(3): 958. doi:10.1002/hep.26327.

Siuffi-Campo, Suad, Ricardo Londoño-García, Yeinis Paola Espinosa-Herrera, Juan Camilo Pérez-Cadavid, and Octavio G. Muñoz-Maya. 2022. "Deficiencia de Lipasa Ácida Lisosomal, Una Enfermedad Subdiagnosticada. Reporte de Caso." *Hepatología*: 97–105. doi:10.52784/27112330.151.

Soeki, Takeshi, and Masataka Sata. 2016. "Inflammatory Biomarkers and Atherosclerosis." *International Heart Journal* 57(2): 134–39. doi:10.1536/ihj.15-346.

Strebinger, Georg, Elena Müller, Alexandra Feldman, and Elmar Aigner. 2019. "<p>Lysosomal Acid Lipase Deficiency – Early Diagnosis Is the Key</P>." *Hepatic Medicine: Evidence and Research* Volume 11: 79–88. doi:10.2147/HMER.S201630.

Viana-Huete, Vanesa, and José J. Fuster. 2019. "Valor Terapéutico Potencial de Las Estrategias Dirigidas Contra La Interleucina 1β En La Enfermedad Cardiovascular Ateroesclerótica." *Revista Española de Cardiología* 72(9): 760–66. doi:10.1016/j.recesp.2019.02.021.

Wilson, Don P., and Nivedita Patni. 2000. *Lysosomal Acid Lipase Deficiency*.

Zhao, Yunyun, Yongjiang Qian, Zhen Sun, Xinyi Shen, Yaoyao Cai, Lihua Li, and Zhongqun Wang. 2021. "Role of PI3K in the Progression and Regression of Atherosclerosis." *Frontiers in Pharmacology* 12. doi:10.3389/fphar.2021.632378.

10. ANNEX I

IISPV
INSTITUT D'INVESTIGACIÓ SANITÀRIA PERE VIRGILI

CEIm
Comitè Ètic d'Investigació amb medicaments

DICTAMEN COMITÉ ÉTICO DE INVESTIGACIÓN CON MEDICAMENTOS

FRANCESC XAVIER SUREDA BATLLE, Secretario del Comité Ético de Investigación con Medicamentos del IISPV da fe de los acuerdos aprobados con el visto bueno de JOSEP MARIA ALEGRET COLOMÉ que preside la reunión.

Este Comité, en su reunión de fecha **24/04/2025** acta número **006/2025** se ha evaluado y decidido emitir **Informe Favorable** para que se realice el estudio titulado:

"Avaluació del paper de la lipasa àcida lisosomal en la progressió de l'aterosclerosi"

Código: ---
Versión Protocolo: S/V
Versión H.I.P. y Consentimiento Informado: s/v
Promotor: INVESTIGADOR
Ref. CEIM: 136/2025

CONSIDERA QUE:

- Se cumplen los requisitos necesarios de idoneidad del protocolo en relación con los objetivos del estudio y están justificados los riesgos y molestias previsibles para el sujeto.
- La capacidad del investigador y los medios disponibles son apropiados para lleva a cabo el estudio.
- Son adecuados tanto el procedimiento para obtener el consentimiento informado como la compensación prevista para los sujetos por daños que pudieran derivarse de su participación en el estudio
- El alcance de las compensaciones económicas previstas no interfiera con el respeto a los postulados éticos.

Este comité **acepta** que dicho estudio sea realizado en:

UNIVERSITAT ROVIRA I VIRGILI por RIBALTA VIVES , JOSEP

En el caso que se evalúe algún proyecto en el que participe como investigador/colaborador algún miembro de este comité, se ausentará de la reunión durante la discusión del estudio.

La composición actual del CEIm del Instituto d'Investigació Sanitària Pere Virigili es la siguiente:

Presidente

Dr. Josep Mª Alegret Colomé
Cardiólogo. *Salut Sant Joan de Reus-Baix Camp.*

Vicepresidente

Dra. Maria Teresa Auguet Quintilla

Registre de Fundacions de la Generalitat de Catalunya núm. inscripció 2.206 – NIF G43814045

1 / 2

Generalitat de Catalunya · S/ICS · S/HJ23 Hospital Universitari Joan XXIII ICS Camp de Tarragona · S/HTVC Hospital de Tortosa Verge de la Cinta · Salut/ Salut Sant Joan Reus - Baix Camp · GRUP PERE MATA · UNIVERSITAT ROVIRA I VIRGILI

www.iispv.cat

Figure 30. Ethical committee's decision accepted to carry out the project.

11.ANNEX II

Lipoprotein profile (Liposcale Test)

Sample ID Client	VLDL-C	IDL-C	LDL-C
LAL-D (Day 1)	5,73	8,79	147,41
LAL-D (Day 7)	4,11	8,59	152,13
LAL-D (Day 14)	4,25	6,95	134,06
Control (Day 1)	9,22	4,99	125,87
Control (Day 7)	9,94	5,27	119,28
Control (Day 14)	6,74	6,05	123,71

Table 8. Cholesterol (mg/dL)

Sample ID Client	VLDL-TG	IDL-TG	LDL-TG
LAL-D (Day 1)	37,89	8,47	15,89
LAL-D (Day 7)	32,82	7,99	15,49
LAL-D (Day 14)	32,11	7,69	12,78
Control (Day 1)	55,76	6,53	10,61
Control (Day 7)	50,33	7,40	10,09
Control (Day 14)	40,88	7,24	10,51

Table 9. Triglycerides (mg/dL)

Sample ID Client	VLDL-P (nmol/L)	Large VLDL-P (nmol/L)	Medium VLDL-P (nmol/L)	Small VLDL-P (nmol/L)
LAL-D (Day 1)	25,46	0,68	3,31	21,47
LAL-D (Day 7)	22,02	0,66	2,44	18,92
LAL-D (Day 14)	22,57	0,60	1,86	20,10
Control (Day 1)	37,38	1,04	4,62	31,72
Control (Day 7)	33,35	0,86	5,57	26,91
Control (Day 14)	26,37	0,74	4,54	21,10

Table 10. VLDL Particle number (P)

Sample ID Client	LDL-P (nmol/L)	Large LDL-P (nmol/L)	Medium LDL-P (nmol/L)	Small LDL-P (nmol/L)
LAL-D (Day 1)	1315,13	263,31	508,07	543,75
LAL-D (Day 7)	1377,65	253,79	531,82	592,04
LAL-D (Day 14)	1248,95	228,53	401,89	618,53
Control (Day 1)	1170,88	221,39	337,78	611,72
Control (Day 7)	1123,53	201,83	322,18	599,52
Control (Day 14)	1130,99	229,00	327,38	574,61

Table 11. LDL Particle number (P)

Sample ID Client	HDL-P (µmol/L)	Large HDL-P (µmol/L)	Medium HDL-P (µmol/L)	Small HDL-P (µmol/L)
LAL-D (Day 1)	25,13	0,34	12,54	12,25
LAL-D (Day 7)	25,42	0,33	12,31	12,78
LAL-D (Day 14)	27,22	0,30	12,80	14,12
Control (Day 1)	26,75	0,29	12,49	13,97
Control (Day 7)	27,43	0,26	10,86	16,31
Control (Day 14)	24,13	0,27	11,06	12,80

Table 12. HDL Particle number (P)

Sample ID Client	VLDL-Z (nm)	LDL-Z (nm)	HDL-Z (nm)
LAL-D (Day 1)	42,39	21,77	8,47
LAL-D (Day 7)	42,29	21,63	8,44
LAL-D (Day 14)	42,00	21,39	8,42
Control (Day 1)	42,35	21,32	8,41
Control (Day 7)	42,67	21,23	8,32
Control (Day 14)	42,75	21,44	8,40

Table 13. Particle diameter (Z)

Glycoprotein profile (Glycoscale Test)

Sample ID Client	Glyc-B (µmol/L)	Glyc-F (µmol/L)	Glyc-A (µmol/L)	H/W Glyc-B	H/W Glyc-A	Glyc-B (µmol/L)
LAL-D (Day 1)	275,69	185,62	543,34	3,47	14,18	275,69
LAL-D (Day 7)	279,85	181,10	504,76	3,52	13,53	279,85
LAL-D (Day 14)	268,26	147,45	481,54	3,37	12,52	268,26
Control (Day 1)	280,69	198,12	602,57	3,53	14,73	280,69
Control (Day 7)	338,40	162,29	633,04	4,25	15,92	338,40
Control (Day 14)	294,07	163,21	547,96	3,70	14,38	294,07

Table 14. Glycoscale Test.

12. ANNEX III

Western Blot: Protein expression quantification tables

	LRP1 Average intensity	Actin Average intensity	Ratio LRP1/Actin (AU)	Fold Change
VLDL Day 1 (100µL)	9356,35	11402,36	0,82	0,97
VLDL Day 7 (100µL)	9529,59	10067,39	0,95	1,49
VLDL Day 14 (100µL)	7222,50	12495,21	0,58	1,20
LDL Day 1 (100µL)	11207,04	12234,44	0,92	1,09
LDL Day 7 (100µL)	9621,49	11351,38	0,85	1,33
LDL Day 14 (100µL)	10113,69	15815,49	0,64	1,33
Control Day 1	9836,61	11659,18	0,84	1
Control Day 7	6188,90	9732,62	0,64	1
Control Day 14	5154,69	10730,30	0,48	1

Table 15. Quantification of LRP1 expression in macrophages from a healthy individual under different lipoprotein incubation conditions and time points. Average band intensities for LRP1 and actin were measured by ImageQuant from Western blot analysis and the intensity was quantified using ImageJ software.. The ratio of LRP1 to actin was calculated for each condition and expressed in arbitrary units (AU). Fold change values were determined by normalizing each condition to the corresponding untreated control at the same time point (set as 1).

	LRP1 Average intensity	Actin Average intensity	Ratio LRP1/Actin (AU)	Fold Change
VLDL Day 1 (100µL)	5046,90	7861,31	0,64	1,11
VLDL Day 7 (100µL)	3829,18	5940,42	0,64	1,10
VLDL Day 14 (100µL)	5469,83	7140,72	0,77	1,44
LDL Day 1 (100µL)	5726,43	7238,36	0,79	1,37
LDL Day 7 (100µL)	4815,97	6459,94	0,75	1,27
LDL Day 14 (100µL)	5934,82	7520,81	0,79	1,49
Control Day 1	3640,85	6315,70	0,58	1
Control Day 7	3920,89	6683,92	0,59	1
Control Day 14	4006,84	7548,46	0,53	1

Table 16. Quantification of LRP1 expression in macrophages from a LAL-D patient under different lipoprotein incubation conditions and time points. Average band intensities for LRP1 and actin were measured by ImageQuant from Western blot analysis and the intensity was quantified using ImageJ software. The ratio of LRP1 to actin was calculated for each condition and expressed in arbitrary units (AU). Fold change values were determined by normalizing each condition to the corresponding untreated control at the same time point (set as 1).

	IL1-B Average intensity	Actin Average intensity	Ratio IL1-B/Actin (AU)	Fold Change
VLDL Day 1 (100µL)	8306,16	7861,31	1,06	1,62
VLDL Day 7 (100µL)	3770,41	5940,42	0,63	2,32
VLDL Day 14 (100µL)	3343,78	7140,72	0,47	2,05
LDL Day 1 (100µL)	6019,25	7238,36	0,83	1,27
LDL Day 7 (100µL)	4578,12	6459,94	0,71	2,58
LDL Day 14 (100µL)	2959,21	7520,81	0,39	1,72
Control Day 1	4129,25	6315,7	0,65	1
Control Day 7	1832,51	6683,92	0,27	1
Control Day 14	1725,71	7548,46	0,23	1

Table 17. Quantification of IL-1β expression in macrophages from a healthy individual under different lipoprotein incubation conditions and time points. Average band intensities for IL-1β and actin were measured by ImageQuant from Western blot analysis and the intensity was quantified using ImageJ software. The ratio of IL-1β to actin was calculated for each condition and expressed in arbitrary units (AU). Fold change values were determined by normalizing each condition to the corresponding untreated control at the same time point (set as 1).

	IL1-B Average intensity	Actin Average intensity	Ratio IL1-B/Actin (AU)	Fold Change
VLDL Day 1 (100µL)	3261,08	7861,31	0,41	1,19
VLDL Day 7 (100µL)	1606	5940,42	0,27	0,98
VLDL Day 14 (100µL)	2796,49	7140,72	0,39	1,64
LDL Day 1 (100µL)	1932,8	7238,36	0,27	0,77
LDL Day 7 (100µL)	1498,8	6459,94	0,23	0,84
LDL Day 14 (100µL)	1641,83	7520,81	0,22	0,91
Control Day 1	2203,16	6315,7	0,35	1
Control Day 7	1843,4	6683,92	0,28	1
Control Day 14	1804,31	7548,46	0,24	1

Table 18. Quantification of IL-1β expression in macrophages from a LAL-D patient under different lipoprotein incubation conditions and time points. Average band intensities for IL-1β and actin were measured by ImageQuant from Western blot analysis and the intensity was quantified using ImageJ software. The ratio of IL-1β to actin was calculated for each condition and expressed in arbitrary units (AU). Fold change values were determined by normalizing each condition to the corresponding untreated control at the same time point (set as 1).